
FIG. 4. Axial (a), mid-sagittal (b), and coronal MRI (c) of a 50-month-old female with *CASK* mutation (Patient 11). Note the microcephaly (a), hypoplastic pons (b), cerebellar hemispheres (c) and vermis (b) with normal appearance of the corpus callosum (a,b).

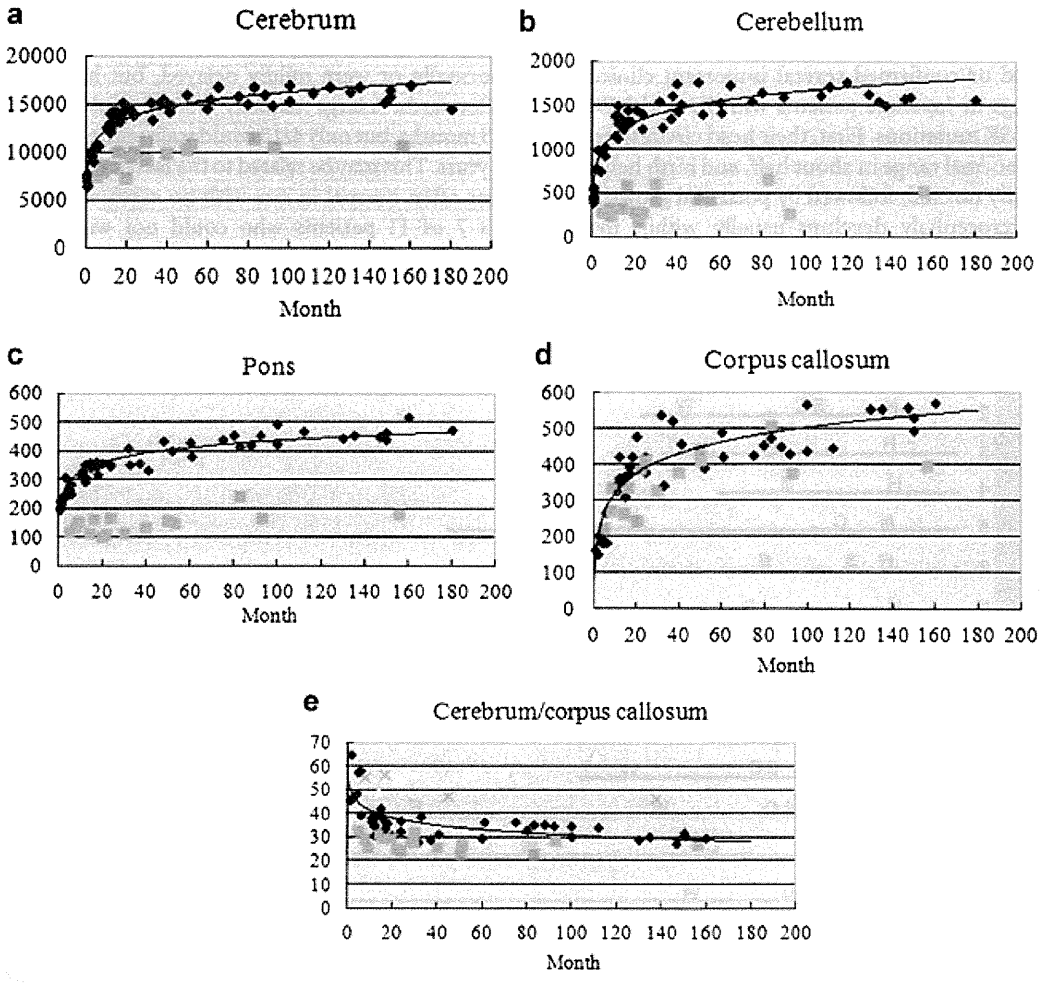


FIG. 5. Longitudinal changes in the cerebrum (a), cerebellar hemisphere (b), pons (c), and corpus callosum (d) areas, along with the cerebrum/corpus callosum area ratio (e). Diamonds represent control patients, squares patients with *CASK* mutations, triangles (e) the patient with PEHO syndrome, and Xs (e) the patients with other pontocerebellar malformations. The relatively normal callosal size combined with reduced size of other structures, resulting in the small cerebrum/corpus callosum ratio, appears to be a fairly unique characteristic of patients with *CASK* mutations.

evaluation were younger than 6 years, some might be expected to acquire this ability in the future.

Epilepsy was present in more than half of the females (53%) in this series, which is more frequent than the previously reported frequency (32%; 8/25) in European countries [Moog et al., 2011]. Seizure onset was between 17 and 130 months (mean, 60 months), and the epilepsy syndrome or seizure type was variable, similar to the previous report of onset at 1–8 years with various types of seizures [Moog et al., 2011]. Because most females without epilepsy were less than 6 years old, the frequency of epilepsy may be higher at subsequent re-evaluations. Child neurologists should be aware that epilepsy associated with ID and MICPCH due to *CASK* mutations has a relatively late onset. The neurological symptoms or facial features in the females were similar to those reported in European patients [Moog et al., 2011], however, hypohidrosis and hyposensitivity to pain were previously unrecognized. Although further clinical study is necessary to evaluate the frequency or severity of hypohidrosis and hyposensitivity to pain, ID and MICPCH associated with *CASK* mutations should be considered in the differential diagnosis of these symptoms.

The MRI findings in this case series confirmed the previous report of a normal to low-normal size of the corpus callosum and a low cerebrum/corpus callosum ratio with reduced areas of the cerebrum, pons, and cerebellar hemispheres. As five disease controls with pontine hypoplasia showed thinning of the corpus callosum and a high cerebrum/corpus callosum ratio, the normal size of the corpus callosum relative to a small cerebrum, which gives an impression of callosal thickening, is an important imaging clue for *CASK* mutations.

The growth pattern, neurologic development, neurological symptoms, and facial features were similar in the 15 females with loss-of-function mutations, which corresponds to previous reports showing that mutations resulting in a null allele are associated with a characteristic pattern of ID and MICPCH in females [Moog et al., 2011; Hayashi et al., 2012]. The one male in this study showed similar growth pattern, facial appearance, and MRI findings to the female patients; however, his neurologic manifestations were more severe, with no motor development and early onset, intractable epilepsy. Though it has been reported that *CASK* missense mutations in males can cause milder phenotypes, such as mild to severe ID with or without nystagmus, microcephaly, and/or dysmorphic features [Hackett et al., 2010] or FG syndrome [Piluso et al., 2009], their clinical features are distinct from ID and MICPCH. FG syndrome entails relative macrocephaly, agenesis of the corpus callosum, and mild ID with congenital nystagmus; microcephaly or cerebellar hypoplasia is rare. The striking difference in clinical severity between the two groups of *CASK* mutations might be explained by the different nature of the mutations; hypomorphic missense mutations in males are likely to have a relatively mild impact on protein structure and function, thus leading to less severe phenotype than the null mutations in females. Null mutations of *CASK* in males would be expected to cause a more severe phenotype than in female patients, usually resulting in prenatal or neonatal lethality. A partly penetrant *CASK* splice site mutation was reported in a severely affected male with MICPCH who died at 2 weeks [Najm et al., 2008]. In silico analysis in the present male patient with ID and MICPCH (Patient 16) showed the de novo missense mutation likely damaged and affected protein function with no splice site disruption, however, the functional CASK studies will be necessary to confirm the pathogenicity of this mutation. To clarify the details of clinical and radiologic features, it would be important to evaluate *CASK* in males with severe psychomotor delay and the characteristic facial appearance or MRI findings.

## ACKNOWLEDGMENTS

We thank the patients and families for their contribution to this study.

## REFERENCES

Hackett A, Tarpey PS, Licata A, Cox J, Whibley A, Boyle J, Rogers C, Grigg J, Partington M, Stevenson RE, Tolmie J, Yates JR, Turner G, Wilson M, Futreal AP, Corbett M, Shaw M, Gecz J, Raymond FL, Stratton MR, Schwartz CE, Abidi FE. 2010. CASK mutations are frequent in males and cause X-linked nystagmus and variable XLMR phenotypes. Eur J Hum Genet 18:544–552.

Hayashi S, Mizuno S, Migata O, Okuyama T, Makita Y, Hata A, Imoto I, Inazawa J. 2008. The *CASK* gene harbored in a deletion detected by array-CGH as a potential candidate for a gene causative of X-linked dominant mental retardation. Am J Med Genet Part A 146A:2145–2151.

Hayashi S, Okamoto N, Chinen Y, Takanashi J, Makita Y, Hata A, Imoto I, Inazawa J. 2012. Novel intragenic duplications and mutations of CASK in patients with mental retardation and microcephaly with pontine and cerebellar hypoplasia (MICPCH). Hum Genet 131:99–110.

Hsueh YP. 2006. The role of the MAGUK protein CASK in neural development and synaptic function. Curr Med Chem 13:1915–1927.

Hsueh YP. 2009. Calcium/calmodulin-dependent serine protein kinase and mental retardation. Ann Neurol 66:438–443.

Moog U, Kutsche K, Kortüm F, Chilian B, Bierhals T, Apeshiotis N, Balg S, Chassaing N, Coubes C, Das S, Engels H, Van Esch H, Grasshoff U, Heise M, Isidor B, Jarvis J, Koehler U, Martin T, Oehl-Jaschkowitz B, Ortibus E, Pilz DT, Prabhakar P, Rappold G, Rau I, Rettenberger G, Schlüter G, Scott RH, Shoukier M, Wohlleber E, Zirn B, Dobyns WB, Uyanik G. 2011. Phenotypic spectrum associated with CASK loss-of-function mutations. J Med Genet 48:741–751.

Najm J, Horn D, Wimplinger I, Golden JA, Chizhikov VV, Sudi J, Christian SL, Ullmann R, Kuechler A, Haas CA, Flubacher A, Charnas LR, Uyanik G, Frank U, Klopocki E, Dobyns WB, Kutsche K. 2008. Mutations of *CASK* cause an X-linked brain malformation phenotype with microcephaly and hypoplasia of the brainstem and cerebellum. Nat Genet 40:1065–1067.

Ninchoji J, Takanashi J. 2010. Pontine hypoplasia in 5p- syndrome; a key MRI finding for a diagnosis. Brain Dev 32:571–573.

Piluso G, D'Amico F, Saccone V, Bismuto E, Rotundo IL, Di Domenico M, Aurino S, Schwartz CE, Neri G, Nigro V. 2009. A missense mutations in *CASK* causes FG syndrome in an Italian family. Am J Hum Genet 84:162–177.

Takanashi J, Arai H, Nabatame S, Hirai S, Hayashi S, Inazawa J, Okamoto N, Barkovich AJ. 2010. Neuroradiological features of *CASK* mutations. AJNR Am J Neuroradiol 31:1619–1622.

Tanaka M, Tanaka Y, Hamano S, Nara T, Imai M. 1997. A case of PEHO (progressive encephalopathy with edema, hypsarrhythmia and optic atrophy) syndrome: Changes in clinical and neuroradiological findings. (In Japanese) No To Hattatsu 29:488–493.

RESEARCH ARTICLE

AMERICAN JOURNAL OF medical genetics

# The Incidence of Hypoplasia of the Corpus Callosum in Patients With dup (X)(q28) Involving *MECP2* Is Associated With the Location of Distal Breakpoints

**Shozo Honda,[1,2] Shin Hayashi,[1,2,3] Takaya Nakane,[4] Issei Imoto,[1,5] Kenji Kurosawa,[6] Seiji Mizuno,[7] Nobuhiko Okamoto,[8] Mitsuhiro Kato,[9] Hiroshi Yoshihashi,[10] Takeo Kubota,[11] Eiji Nakagawa,[12,13] Yu-ichi Goto,[12,13] and Johji Inazawa[1,2,3,14]***

[1]Department of Molecular Cytogenetics, Medical Research Institute and School of Biomedical Science, Tokyo Medical and Dental University, Bunkyo-ku, Tokyo, Japan

[2]21st Century Center of Excellence Program for Molecular Destruction and Reconstitution of Tooth and Bone, Tokyo Medical and Dental University, Bunkyo-ku, Tokyo, Japan

[3]Hard Tissue Genome Research Center, Tokyo Medical and Dental University, Bunkyo-ku, Tokyo, Japan

[4]Faculty of Medicine, Department of Pediatrics, University of Yamanashi, Chuo, Yamanashi, Japan

[5]Department of Human Genetics and Public Health, Graduate School of Medical Science, The University of Tokushima, Tokushima, Japan

[6]Kanagawa Children's Medical Center, Division of Medical Genetics, Minami-ku, Yokohama, Japan

[7]Aichi Human Service Center, Department of Pediatrics, Central Hospital, Kasugai, Aichi, Japan

[8]Department of Medical Genetics, Osaka Medical Center and Research Institute for Maternal and Child Health, Izumi, Osaka, Japan

[9]Department of Pediatrics, Yamagata University School of Medicine, Yamagata, Japan

[10]The Division of Medical Genetics, Tokyo Metropolitan Children's Medical Center, Fuchu, Tokyo, Japan

[11]Department of Epigenetics Medicine, Interdisciplinary Graduate School of Medicine and Engineering, University of Yamanashi, Chuo, Yamanashi, Japan

[12]Department of Child Neurology, National Center Hospital, National Center of Neurology and Psychiatry (NCNP), Kodaira, Tokyo, Japan

[13]Department of Mental Retardation and Birth Defect Research, National Institute of Neuroscience, NCNP, Kodaira, Tokyo, Japan

[14]Core Research for Evolutional Science and Technology (CREST) of Japan Science and Technology Corporation (JST), Saitama, Japan

Manuscript Received: 6 December 2010; Manuscript Accepted: 23 January 2012

Duplications of Xq28 harboring the methyl CpG binding protein 2 (*MECP2*) gene explain approximately 1% of X-linked mental disability (XLMR). The common clinical features observed in patients with dup(X)(q28) are severe ID, infantile hypotonia, mild dysmorphic features and a history of recurrent infections and *MECP2* duplication syndrome is now recognized as a clinical entity. While some patients with this syndrome have other characteristic phenotypes, the reason for the spectrum of phenotypes has not been clarified. Since dup(X)(q28) rearrangements vary in size and location, genes other than *MECP2* might affect the phenotype. We used a high-density oligonucleotide

How to Cite this Article:
Honda S, Hayashi S, Nakane T, Imoto I, Kurosawa K, Mizuno S, Okamoto N, Kato M, Yoshihashi H, Kubota T, Nakagawa E, Goto Y-i, Inazawa J. 2012. The incidence of hypoplasia corpus callosum in patients with dup (X)(q28) involving *MECP2* is associated with the location of distal breakpoints.
Am J Med Genet Part A 158A:1292–1303.

Additional supporting information may be found in the online version of this article.

Grant sponsor: Ministry of Education, Culture, Sports, Science and Technology, Japan; New Energy and Industrial Technology Development Organization (NEDO); Ministry of Health, Labor and Welfare, Japan; Joint Usage/Research of Medical Research Institute, Tokyo Medical Dental University; Research Fellowship of the Japan Society for the Promotion of Science (JSPS) for Young Scientists.

*Correspondence to:
Johji Inazawa, M.D., Ph.D., Department of Molecular Cytogenetics, Medical Research Institute, Tokyo Medical and Dental University, Yushima 1-5-45, Bunkyo-ku, Tokyo 113-8510, Japan.
E-mail: johinaz.cgen@mri.tmd.ac.jp

Article first published online in Wiley Online Library (wileyonlinelibrary.com): 23 April 2012
DOI 10.1002/ajmg.a.35321

array to carry out precise mapping in eight Japanese families in which dup(X)(q28) was detected using an in-house bacterial artificial chromosome-based microarray in seven cohorts of individuals with multiple congenital anomalies and intellectual disability (MCA/ID) or with XLID. We hypothesized that the size, gene content, and location of dup(X)(q28) may contribute to variable expressivity observed in *MECP2* duplication syndrome. Genotype–phenotype correlation in our cases together with cases reported in the literature suggested that copy number gains between two low copy repeats (LCRK1 and LCRL1) are associated with the incidence of hypoplasia of the corpus callosum. Further studies are necessary to understand the mechanism of this association.

Key words:

## INTRODUCTION

Duplications at Xq28 encompassing the methyl CpG binding protein 2 gene (*MECP2*) (OMIM:300005) have been detected at high frequency (1–2%) in cohorts of males with unexplained X-linked intellectual disability (XLID) [Lugtenberg et al., 2009; Honda et al., 2010]. *MECP2* duplication syndrome (OMIM:300260) is now recognized as a clinical entity characterized by severe ID, progressive spasticity, muscular hypotonia, absence of speech, recurrent infections, and mild dysmorphic features [Ramocki et al., 2010]. In addition, most patients with dup(X)(q28) exhibit other clinical signs, such as delayed acquisition or lack of ambulation, constipation, epilepsy, digital abnormalities, and genital abnormalities [del Gaudio et al., 2006; Bartsch et al., 2010]. These nonrecurrent duplications at Xq28 vary in size (0.1–2.6 Mb), gene content and location, suggesting that specific genes included in the duplication may contribute to the observed phenotypic variability. Although duplications of *IRAK1* (OMIM:300283) and *FLNA* (OMIM:300017) may be responsible for respiratory infections and constipation [Smyk et al., 2008; Clayton-Smith et al., 2009], it has not been clarified yet how location or size is involved or which genes other than *MECP2*, *IRAK1*, and *FLNA* might affect phenotypes.

We constructed bacterial artificial chromosome (BAC)-based arrays and established aCGH systems for the detection of cryptic copy-number variants (CNVs) in the human genome [Inazawa et al., 2004]. Using an in-house BAC-based array system, we screened for pathogenic CNVs in cohorts of patients with multiple congenital anomalies and intellectual disability (MCA/ID) [Hayashi et al., 2007, 2010] and in male patients with unexplained X-linked ID [Takano et al., 2008; Honda et al., 2010], and found dup(X)(q28) encompassing *MECP2* in a total of 12 males from eight families. We hypothesized that the location and the size of the genomic rearrangements influence phenotypes of patients with dup(X)(q28) encompassing *MECP2*. To test this hypothesis, we performed precise mapping studies of the genomic rearrangements using a high-density oligonucleotide array, and we performed a detailed genotype–phenotype correlation studies using both our cases and literature cases. Although genotype–phenotype correlation were not indicated with clarity, this result demonstrated that the incidence of hypoplasia of the corpus callosum (CC) were associated with the location of the distal breakpoints of dup(X)(q28). Further studies are necessary to understand the mechanism of this association and reveal the cause of the hypoplasia of the CC in this patient population.

## MATERIALS AND METHODS

### Patients

From a consortium of 23 medical institutes and hospitals in Japan, we recruited 115 males with MCA/ID of unknown etiology registered from May 2008 to March 2010 [Hayashi et al., 2010]. All samples were obtained with prior written informed consent from the parents and approval by the local ethics committee. Included patients were physically examined by experts in medical genetics or dysmorphology of each institution, and each patient had showed a normal male karyotype on G-band karyotyping at the 400–550 band-level. We identified dup(X)(q28) harboring *MECP2* in each proband in families 64-2-098, 64-5-093, and 81-22-020M using in-house BAC-based arrays [Hayashi et al., 2010].

We also organized an X-linked ID research consortium in Japan, and we have been developing a research resource and biological sample repository since 2003 [Takano et al., 2008; Honda et al., 2010]. We recruited 173 families that include at least one male with unexplained ID. All peripheral blood samples were obtained with informed consent using human subjects research protocols approved by the Institutional Review Board of all institutes. Genomic DNA and metaphase chromosomes were prepared from peripheral blood or from Epstein–Barr virus (EBV)-transformed lymphoblastoid cell lines (LCLs) in accordance with standard procedures. Blood samples from the probands of 173 families were subjected to conventional karyotyping and were found to have a normal male karyotype. We next screened all 173 families using a BAC-based X chromosome-tiling array [Hayashi et al., 2007; Honda et al., 2010]. We identified Xq28 duplications including *MECP2* in four of these families, MRK2M, MRYB6, MR1P3, and MR347. The preliminary mapping of the genomic rearrangements in families, MRYB6, MR1P3, and MR347, was reported elsewhere [Honda et al., 2010]. A fifth family with an Xq28 duplication including, *MECP2* and YU78, was detected by FISH using a BAC probe containing *MECP2*, since the proband and his brother demonstrated some characteristics of patients with *MECP2* duplication syndrome [Meins et al., 2005; Van Esch et al., 2005; Friez et al., 2006; Ramocki et al., 2010]. Total 5/173 (2.89%) of the XLID samples in our repository were positive for Xq28 duplications including *MECP2*.

We identified 11 of these cases and 36 literature cases with *MECP2* duplication in which precise mapping and a magnetic resonance imaging (MRI) head scan had been reported to include our genotype–phenotype correlation studies.

### Array-CGH

Array-CGH hybridization using the MCG X-tiling array [Hayashi et al., 2007] and the MCG Genome Disorder (GD) Array, which

contains 700 BACs covering all subtelomeric regions and regions corresponding to 31 known congenital disorders [Hayashi et al., 2010], was performed as described previously using DNA extracted from sex-matched normal lymphocytes as a reference [Honda et al., 2007]. Precise mapping of each dup(X)(q28) rearrangement was performed using the Agilent Human Genome CGH Microarray 244K (Agilent Technologies, Santa Clara, CA) as reported [Honda et al., 2010].

### FISH

FISH analyses were performed as described previously [Honda et al., 2007], using BAC or PAC clones located around the region of interest as probes.

### The *Androgen Receptor* (*AR*) X-Inactivation Assay

The pattern of X-chromosome inactivation in females was evaluated using the androgen receptor (AR) X-inactivation assay described by Kubota et al. [1999] with minor modifications. Briefly, DNA was modified with sodium bisulfite and amplified with primers specific for methylated or unmethylated DNA sequence at the human *androgen receptor* (*HUMARA*) locus where methylation correlates with X-inactivation. Two different sized products due to triplet repeat polymorphism from the paternal or maternal alleles were amplified and analyzed on a 3130 Genetic Analyzer (Applied Biosystems, Foster City, CA), and peak images of each PCR product were measured with GeneMapper Software v4.0 (Applied Biosystems).

### Late Replication Assay

A late replication assay was performed using a thymidine synchronization, bromodeoxyuridine (BrdU) release technique as reported previously [Inazawa et al., 1993] with minor modifications. Metaphase chromosomes were prepared with addition of BrdU to the culture medium for the last 6 hr of cell culture following thymidine synchronization. The slides were stained with Hoechst 33258 (1 mg/ml; Sigma, Saint Louis, MO) for 5 min, and exposed to 254 nm UV light (Stratalinker UV Crosslinker 1800; Agilent Technologies, Santa Clara, CA) at a distance of 20 cm for 10 min after heating at 75°C for 10 min. These chromosome spreads were used for FISH to estimate the rate of inactivation of the affected X chromosome.

## RESULTS

### Clinical Features of the Families

The pedigrees of five newly identified affected families are provided in Figure 1. The perinatal and developmental histories and clinical data for the probands in eight families are summarized in Table I and in Supplementary eTable SI (see Supporting Information online). Severe ID, absence of speech, muscular hypotonia, recurrent respiratory infections, epilepsy, and apparent loss of cerebral volume are present in greater than 70% of the patients (Table I). Detailed clinical summaries for each of the newly identified families are described below.

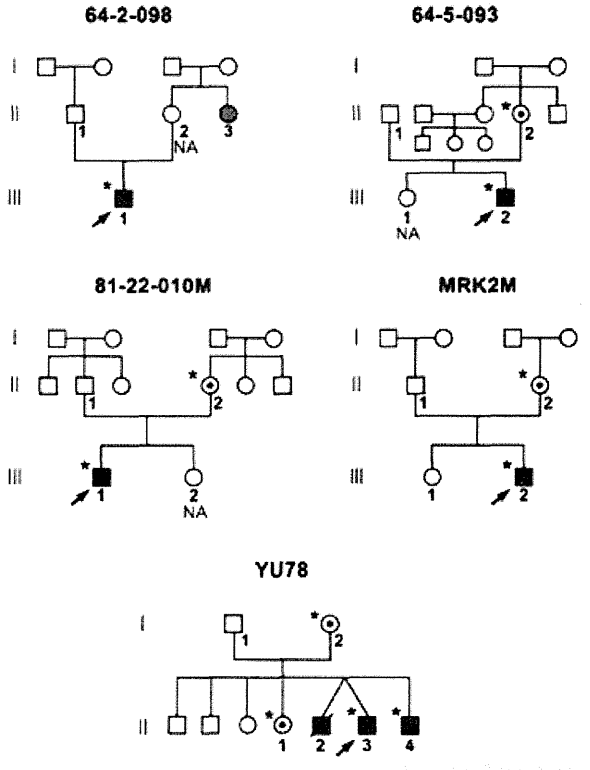


**FIG. 1. Pedigrees of five families with dup(X)(q28) harboring *MECP2*. Closed squares and circles, gray circles, and dotted circles indicate ID, borderline ID, and carriers, respectively. The proband is indicated by arrows. Asterisks indicate persons harboring the *MECP2* duplication within each family. A slash indicates that the person has died. NA, not available.**

### Family 64-2-098

The proband (III-1) was born by normal vaginal delivery after an uneventful pregnancy to nonconsanguineous healthy parents. His weight was 2,412 g (−2.4 SD) and OFC was 32 cm (−1.3 SD) at birth. His mother's younger sister (II-3) has moderate ID and graduated from a school for disabled children (Fig. 1A). He has microcephaly and short stature. At 14 months, his height, weight, and OFC were 64.5 cm (−4.8 SD), 7.7 kg (−1.9 SD), and 42 cm (−2.7 SD), respectively. His development was delayed; at 17 months he first started smiling and could support his head, and he could not roll over at 2 years of age. MRI of the brain showed apparent loss of cerebellum and cerebral volume, hypoplasia of the CC (Fig. 2), and delayed myelination. He exhibited strong autistic behavior and facial dysmorphism. A blood sample from his mother (II-1) was not available for testing.

### Family 64-5-093

The proband (III-2) was born via normal vaginal delivery after an uneventful pregnancy to nonconsanguineous healthy parents. His weight was 2,635 g (−1.8 SD) and his OFC was 34.5 cm (0.6 SD) at

TABLE I. Summary of Clinical Findings in Eight Families Having the Duplication at Xq28

| | No. of patients with symptom/total no. in group [Honda et al., 2010] | | | | | | | | |
|---|---|---|---|---|---|---|---|---|---|
| | 64-2-098 | 64-5-093 | 81-22-010M | MRK2M | YU78 | MRYB6 | MR1P3 | MR347 | n/N (%) |
| Clinical features | | | | | | | | | |
| Mental retardation | 1/1 | 1/1 | 1/1 | 1/1 | 3/3 | 2/2 | 1/1 | 2/2 | 12/12 (100) |
| Muscular hypotonia | 1/1 | 1/1 | 0/1 | 0/1 | 3/3 | 2/2 | 1/1 | 2/2 | 10/12 (83) |
| Absent speech | 1/1 | 1/1 | 1/1 | 1/1 | 3/3 | 2/2 | 1/1 | 2/2 | 12/12 (100) |
| Recurrent respiratory infection | 1/1 | 0/1 | 1/1 | 0/1 | 3/3 | 2/2 | 1/1 | 2/2 | 10/12 (83) |
| Pneumonia | 1/1 | 0/1 | 1/1 | 0/1 | 3/3 | 2/2 | 1/1 | 0/2 | 8/12 (67) |
| Lack of ambulation | 1/1 | 0/1a | 0/1 | 0/1 | 3/3 | 2/2 | 1/1 | 0/2[b] | 7/12 (58) |
| Epilepsy | 0/1 | 0/1 | 0/1 | 1/1 | 3/3 | 2/2 | 1/1 | 2/2 | 9/12 (75) |
| Spasticity | 0/1 | 0/1 | 0/1 | 1/1 | 3/3 | 0/2 | 0/1 | 2/2 | 6/12 (50) |
| Swallowing dysfunction | 1/1 | 0/1 | 0/1 | 0/1 | 3/3 | 2/2 | 1/1 | 0/2 | 7/12 (58) |
| Autistic feature | 1/1 | 1/1 | 0/1 | ND | 0/3 | 2/2 | 1/1 | 2/2 | 7/11 (64) |
| Gastroesophageal reflux | 1/1 | 0/1 | 0/1 | 0/1 | 2/3 | 0/2 | 1/1 | 0/2 | 4/12 (33) |
| Bronchitis | 1/1 | 0/1 | 0/1 | 0/1 | 3/3 | 2/2 | 1/1 | 0/2 | 7/12 (58) |
| Cyanosis | 0/1 | 0/1 | 0/1 | 0/1 | 1/3 | 1/2 | 0/1 | 0/2 | 2/12 (17) |
| Constipation | 1/1 | 1/1 | 0/1 | 0/1 | 2/3 | 2/2 | 1/1 | 0/2 | 7/12 (58) |
| Abdominal distension | 0/1 | 0/1 | 0/1 | 0/1 | 2/3 | 0/2 | 0/1 | 0/2 | 2/12 (17) |
| Otitis media | 0/1 | 0/1 | 1/1 | 0/1 | 2/3 | 0/2 | 0/1 | 0/2 | 3/12 (25) |
| Osteoporosis | 0/1 | 0/1 | 1/1 | 0/1 | 0/3 | 0/2 | 0/1 | 0/2 | 1/12 (8) |
| Brisk tendon replex | 0/1 | 0/1 | 0/1 | 1/1 | 0/3 | 2/2 | 1/1 | 2/2 | 6/12 (50) |
| Dysmorphic features | | | | | | | | | |
| Macrocephaly | 0/1 | 0/1 | 0/1 | 0/1 | 0/3 | 1/2 | 0/1 | 0/2 | 1/12 (8) |
| Microcephaly | 1/1 | 0/1 | 1/1 | 0/1 | 1/3 | 0/2 | 0/1 | 0/2 | 3/12 (25) |
| Plagiocephaly | 0/1 | 0/1 | 1/1 | 0/1 | 0/3 | 0/2 | 0/1 | 2/2 | 3/12 (25) |
| Flat occiput | 1/1 | 0/1 | 0/1 | 0/1 | 0/3 | 0/2 | 0/1 | 0/2 | 1/12 (8) |
| Frontal bossing | 1/1 | 0/1 | 0/1 | 0/1 | 0/3 | 0/2 | 0/1 | 0/2 | 1/12 (8) |
| Hypotonic face | 0/1 | 0/1 | 0/1 | 0/1 | 1/3 | 0/2 | 0/1 | 0/2 | 1/12 (8) |
| Flat face | 1/1 | 0/1 | 0/1 | 0/1 | 2/3 | 0/2 | 0/1 | 0/2 | 3/12 (25) |
| Round and expression-less face | 1/1 | 1/1 | 0/1 | 1/1 | 3/3 | 1/2 | 1/1 | 2/2 | 10/12 (83) |
| Long face | 0/1 | 0/1 | 0/1 | 0/1 | 0/3 | 0/2 | 0/1 | 2/2 | 2/12 (17) |
| Synophrys | 0/1 | 0/1 | 0/1 | 0/1 | 0/3 | 1/2 | 0/1 | 0/2 | 1/12 (8) |
| Downslanted palpebral fissures | 0/1 | 0/1 | 1/1 | 0/1 | 0/3 | 0/2 | 0/1 | 0/2 | 1/12 (8) |
| Epicanthus | 1/1 | 0/1 | 1/1 | 0/1 | 0/3 | 1/2 | 0/1 | 0/2 | 3/12 (25) |
| Short nose | 0/1 | 0/1 | 1/1 | 0/1 | 2/3 | 0/2 | 0/1 | 0/2 | 3/12 (25) |
| Wide and depressed nasal bridge | 1/1 | 0/1 | 1/1 | 0/1 | 3/3 | 0/2 | 1/1 | 0/2 | 6/12 (50) |
| Prominent nasal bridge | 1/1 | 0/1 | 0/1 | 0/1 | 0/3 | 0/2 | 0/1 | 2/2 | 3/12 (25) |
| High palate | 0/1 | 0/1 | 0/1 | 0/1 | 1/3 | 2/2 | 0/1 | 0/2 | 3/12 (25) |
| Open mouth | 1/1 | 0/1 | 0/1 | 0/1 | 1/3 | 0/2 | 1/1 | 2/2 | 5/12 (42) |
| Narrow mouth | 1/1 | 0/1 | 1/1 | 0/1 | 0/3 | 0/2 | 0/1 | 0/2 | 2/12 (17) |
| Narrow palate | 1/1 | 0/1 | 1/1 | 0/1 | 0/3 | 0/2 | 0/1 | 0/2 | 2/12 (17) |
| Thick lips | 0/1 | 0/1 | 0/1 | 1/1 | 0/3 | 0/2 | 1/1 | 2/2 | 4/12 (33) |
| Prognathism | 0/1 | 0/1 | 0/1 | 0/1 | 0/3 | 0/2 | 0/1 | 2/2 | 2/12 (17) |
| Short neck | 1/1 | 0/1 | 0/1 | 0/1 | 0/3 | 0/2 | 0/1 | 0/2 | 1/12 (8) |
| Dysmorphic ears | 1/1 | 0/1 | 0/1 | 0/1 | 0/3 | 0/2 | 0/1 | 0/2 | 1/12 (8) |
| Narrow feet | 0/1 | 0/1 | 0/1 | 0/1 | 0/3 | 1/2 | 0/1 | 0/2 | 1/12 (8) |
| Long fingers and toes | 0/1 | 0/1 | 0/1 | 0/1 | 0/3 | 0/2 | 0/1 | 2/2 | 2/12 (17) |
| Tapering fingers | 1/1 | 0/1 | 0/1 | 1/1 | 3/3 | 2/2 | 0/1 | 0/2 | 7/12 (58) |
| Bilateral cubitus valgus | 0/1 | 0/1 | 0/1 | 0/1 | 0/3 | 1/2 | 0/1 | 0/2 | 1/12 (8) |
| Bilateral cryptorchidism | 1/1 | ND | 0/1 | 0/1 | 0/3 | 2/2 | 0/1 | 0/2 | 3/11 (27) |
| Neuroimaging findings | | | | | | | | | |
| Hypoplasia of the corpus callosum | 1/1 | 0/1 | 1/1 | 0/1 | 2/2 | 2/2 | 0/1 | 0/2 | 6/11 (54) |
| Apparent loss of cerebral volume | 1/1 | 0/1 | 0/1 | 0/1 | 2/2 | 2/2 | 1/1 | 2/2 | 8/11 (73) |
| Apparent loss of cerebellar volume | 1/1 | 0/1 | 0/1 | 0/1 | 0/2 | 2/2 | 0/1 | 0/2 | 3/11 (27) |
| Brain stem atrophy | 0/1 | 0/1 | 0/1 | 0/1 | 0/2 | 2/2 | 0/1 | 0/2 | 2/11 (18) |

[Continued]

TABLE I. (Continued)

| | No. of patients with symptom/total no. in group [Honda et al., 2010] | | | | | | | | |
|---|---|---|---|---|---|---|---|---|---|
| | 64-2-098 | 64-5-093 | 81-22-010M | MRK2M | YU78 | MRYB6 | MR1P3 | MR347 | n/N (%) |
| Ventricular dilatation | 0/1 | 0/1 | 1/1 | 0/1 | 0/2 | 2/2 | 1/1 | 0/2 | 4/11 (36) |
| Cisterna magna dilatation | 0/1 | 0/1 | 1/1 | 0/1 | 0/2 | 0/2 | 0/1 | 0/2 | 1/11 (9) |
| Global dilatation of the subarachnoid space | 0/1 | 0/1 | 1/1 | 0/1 | 0/2 | 0/2 | 0/1 | 0/2 | 1/11 (9) |
| Delayed myelination of the white cortex | 1/1 | 0/1 | 0/1 | 0/1 | 0/2 | 0/2 | 0/1 | 0/2 | 1/11 (9) |
| Ggray matter heterotopia | 0/1 | 0/1 | 1/1 | 0/1 | 0/2 | 0/2 | 0/1 | 0/2 | 1/11 (9) |
| Absent septum pellucidum | 0/1 | 0/1 | 0/1 | 0/1 | 0/2 | 1/2 | 0/1 | 0/2 | 1/11 (9) |
| Septum pellucidum cyst | 0/1 | 0/1 | 1/1 | 0/1 | 0/2 | 1/2 | 0/1 | 0/2 | 2/11 (18) |
| White matter change | 1/1 | 0/1 | 0/1 | 0/1 | 0/2 | 0/2 | 0/1 | 2/2 | 3/11 (27) |

[a]One patient started to walk at 22 months.
[b]Two patients started to walk at 36 and 42 months.

birth. He could support his head at 4 months, sit alone at 8 months, and walk without support at 22 months. He had severe constipation. There are no characteristic dysmorphic features or neurological findings (Fig. 2). His unaffected older sister (III-1) was not available for testing.

### Family 81-22-010M

The proband (II-2) was delivered at 40 weeks gestation via cesarean for fetal distress secondary to hypercoiling of the umbilical cord. His birth height, weight, and OFC were 50 cm (0.1 SD), 2,558 g (−2 SD), and 33 cm (−0.5 SD), respectively. His younger sister (III-2) is normal. He first started smiling at 4 months and was able to support his head at 6 months, roll over at 7 months, sit alone at 14 months, and crawl at 16 months. He was diagnosed with relative microcephaly. An MRI of the brain demonstrated hypoplasia of the CC (Fig. 2), ventricular dilatation, cisterna magna dilatation, global dilatation of the subarachnoid spaces, gray matter heterotopia, and a septum pellucidum cyst.

### MRK2M

The proband (III-2) was born by normal vaginal delivery after an uneventful pregnancy to nonconsanguineous healthy parents. His weight was 2,638 g (−1.8 SD) and OFC was 34.5 cm (0.6 SD) at birth. His elder sister (III-1) is healthy. He was able to support his head at 6 months; sit alone at 10 months; and crawl at 18 months. An MRI of the brain was unremarkable (Fig. 2).

### YU78

The proband (II-3) was born at 37 weeks gestation after an uneventful pregnancy to nonconsanguineous healthy parents as

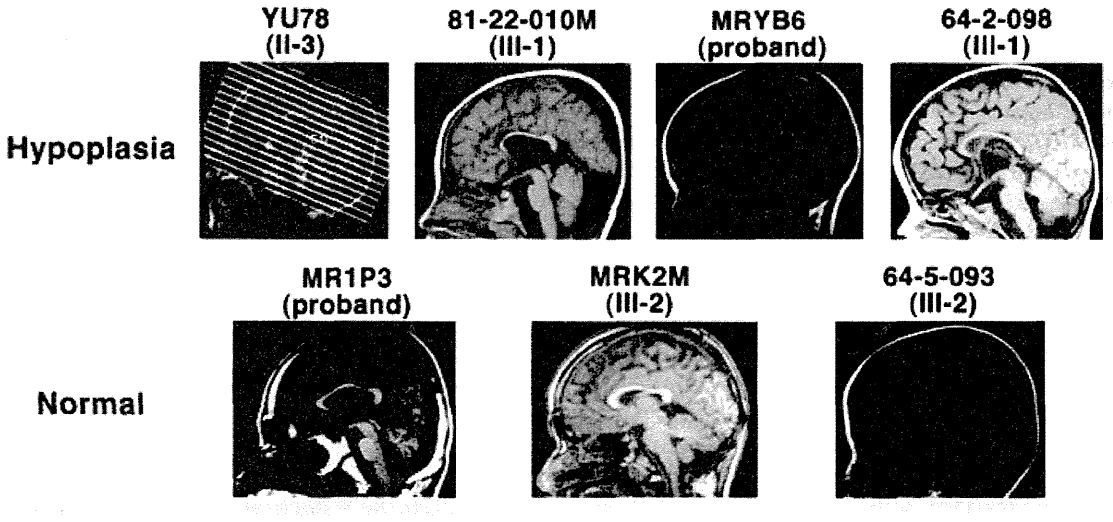


FIG. 2. Brain magnetic resonance images of our patients. The mid-line sagittal T1w sequences show hypoplasia of the corpus callosum in four patients (above) and normal images in three patients (below).

the second of identical twins. The patient had 4 healthy siblings (2 males and 2 females) and 2 affected brothers, his identical twin (II-2) and a younger brother (II-4; Fig. 1E), with similar clinical manifestations. His birth weight was 2,700 g (−0.5 SD), but neither birth height nor OFC was recorded. He could sit alone at the age of 4 months, but at age 19, he could not stand without support nor speak any meaningful words. Seizure onset occurred at 6 years of age, and he was started on an anticonvulsant, which controlled the convulsions well. He exhibited progressive spasticity in his lower legs. At age 19, his weight was 24.5 kg (−4.2 SD), height was 141.0 cm (−5.6 SD), and OFC was 54 cm (−0.7 SD), indicating short stature. He was severely intellectual disabled and so his IQ could not be evaluated. MRI of the brain demonstrated apparent loss of cerebral volume and hypoplasia of the CC (Fig. 2). His identical twin (II-2) followed a similar clinical course. He could roll over, crawl and sit alone, but he could not stand without support or speak any meaningful words. He died at 10 years of age for unknown reasons. MRI analysis has not been performed. The younger brother (II-4) was born at 41 weeks gestation with an uneventful pregnancy and delivery. His birth weight was 3,274 g (−0.3 SD), but neither birth height nor OFC was recorded. He also followed a similar clinical course. His growth and psychological development was severely delayed; he demonstrated hypotonia. He had difficultly feeding due to poor suck/discoordinated swallowing as a neonate. Gastric tube feeding was introduced due to swallowing difficulties at age 5 years. He developed myoclonic epilepsy that proved to be medically refractory. His weight was 22.2 kg (−4.5 SD), height was 139.0 cm (−6.0 SD), and OFC was 51 cm (−2.7 SD) at 17 years of age, indicating short stature. He had microcephaly and progressive spasticity of his lower extremities. MRI of the brain demonstrated apparent loss of cerebral volume and hypoplasia of the CC.

## Precise Mapping dup(Xq28) by aCGH

To determine the size, extent, genomic content, and precise position of the dup(X)(q28) in the proband of each family, we performed aCGH using both the MCG X-tiling array and the oligonucleotide array (Fig. 3). The size of the dup(X)(q28) in each family is summarized in Supplementary eTable SII (see Supporting Information online). In Families 64-2-098, 81-22-010M, and MRK2M, the duplication was respectively described as follows; arr Xq27.3q28(145,477,598–154,913,754)x2, arr Xq28(152,698,840–153,316,250)x2, and arr Xq28 (152,754,271–153,176,409)x2 (Fig. 3A–C). In Family 64-5-093, the dup(X)(q28) contained an ~206 kb triplicated segment (Fig. 3D) involving part of *MECP2* described as arr Xq28(152,754,271–153,003,769x2,153,010,911–153,217,280x3,153,230,084–153,262,357x2). In Family YU78 an ~228 kb triplication at Xp22.2 was detected simultaneously with dup(X)(q28) (Fig. 3E); arr Xp22.2(13,291,526–13,519,924)x3, Xq28(152,494,685–153,067,527)x2. Moreover, we reviewed our previous results for three families (MRYB6, MR1P3, and MR347) and found a triplicated segment embedded in the duplication in MR1P3 and MR347 (Fig. 3F). These aberrations were respectively described as follows; arr Xq28(152,676,750–153,062, 548x2, 153,067,477–153,158,866x3), and arr Xq28(152,721,476–153,062,548x2, 153,067,477–153,217,280x3, 153,230,084–153,266,394x2). A comparison of the dup(X)(q28) rearrangements detected in these eight Japanese families showed that the smallest region of overlap (SRO) was ~220 kb encompassing at least 10 genes including *MECP2* annotated in the UCSC genome browser (NCBI build 36, http://genome.ucsc.edu/cgi-bin/hgGateway; Fig. 4).

## Distal Breakpoints of dup(X)(q28) Are Associated With the Incidence of Hypoplasia of the Corpus Callosum

We compared duplications at Xq28 in the current 11 cases and in 35 cases from the literature. We exhibit the duplicated regions of each patient in the order of the distal boundaries of our cases and the literature cases, respectively (Fig. 4). These results suggest a trend that patients with relatively distal breakpoints are prone to hypoplasia of the CC. In some literature cases of hypoplasia of the CC their distal break points were obscure, thus we classified them according to whether their distal breakpoint involved in LCRL, which was the most distal low copy repeat near *MECP2* [del Gaudio et al., 2006; Carvalho et al., 2009]. Our genotype–phenotype correlation analysis suggests that 83% (10/12) of patients with distal breakpoints near/on/over LCRL demonstrate hypoplasia of the CC, whereas only 17% (6/35) of those with breakpoints proximal to LCRL exhibited hypoplasia of the CC (Fig. 4; Table II).

## FISH Analyses of dup(X)(q28)

Although parental samples for Family 64-2-098 were not available, FISH analysis showed that all mothers for whom we have analyzed carried the same *MECP2* duplication as their sons. In the proband of Family 64-2-098, *MECP2*-specific signals could be detected at Xp24 as well as in situ at Xq28 (Supplementary eFig. S1A). In the other seven families, fluorescent signals specific to *MECP2* were observed only at Xq28, showing that tandem duplication of *MECP2* took place at Xq28 in these families (Supplementary eFig. S1B–E). Interestingly, in YU78, trp(X)(p22.2) and dup(X)(q28) were both observed on the X chromosome in the male proband (YU78, II-2). The same concomitant CNVs were detected in one of two homologous X chromosomes in his carrier mother (YU78, I-2) and in his brother (YU78, II-4) and carrier sister (YU78, II-1; Supplementary eFig. S1E). For three other families (MRYB6, MR1P3, and MR347), FISH results were reported in our recent study [Honda et al., 2010].

## All Carriers Showed a Skewed X-Inactivation Pattern and Dominant Inactivation of the Duplicated Allele

To investigate the X-inactivation status of the unaffected mothers and unaffected sister, we performed the AR X-inactivation assay described by Kubota et al. [1999]. Unaffected carrier mothers in all families showed a skewed X-inactivation pattern. We also

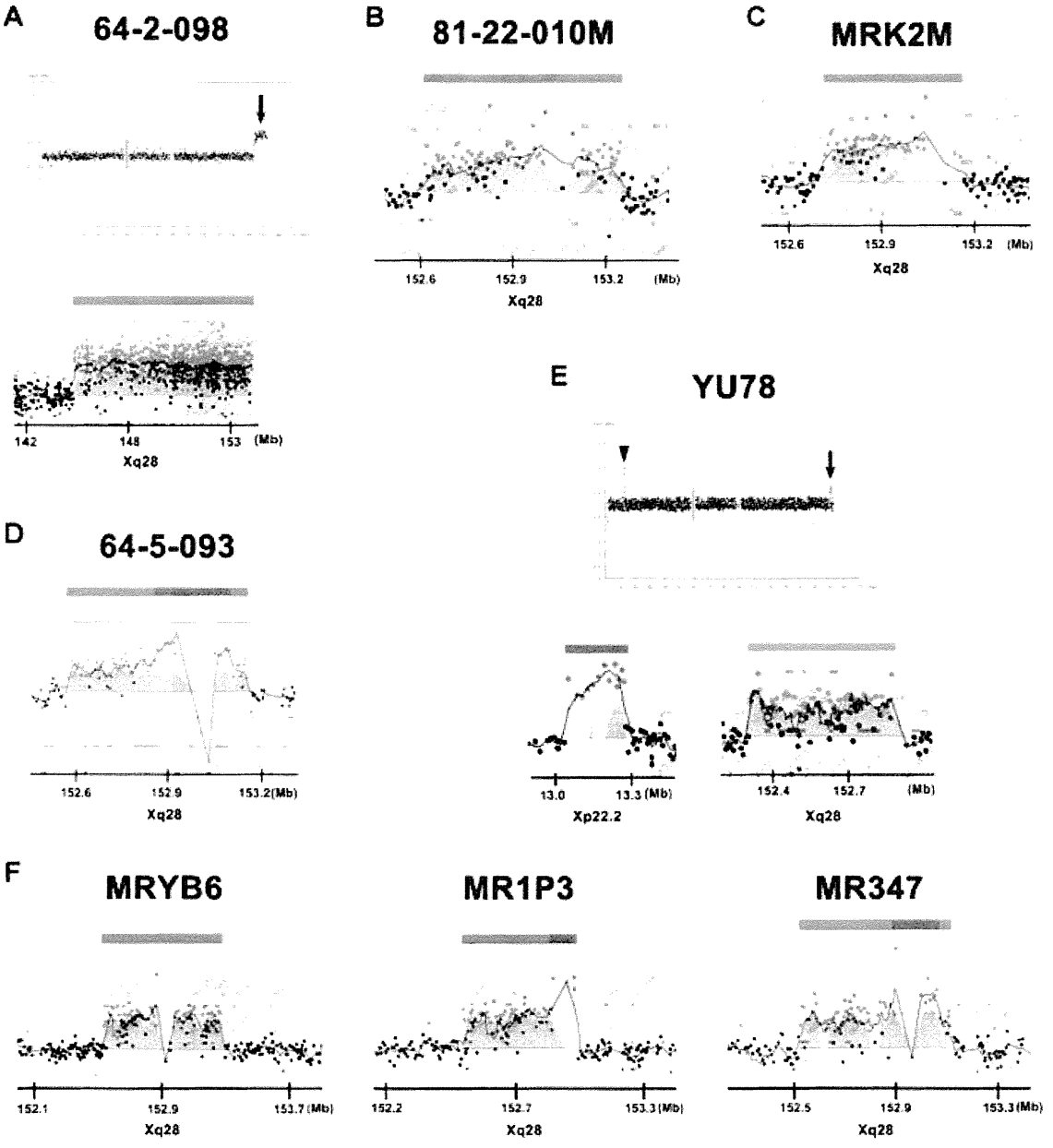


**FIG. 3. Results of the array-CGH analysis with Agilent 244K in probands of eight families carrying *MECP2* duplications. Each dot represents the $\log_2$ ratio of probes on the Agilent 244K array (red: ratio >0.5, green: ratio >1.25, blue: normal ratio). Red and green lines above each diagram represent duplicated and triplicated segments that showed more than three consecutive probes representing an aberrant ratio (duplication: ratio >0.5, triplication: ratio >1.25), respectively. For Families 64-2-098 and YU78, the profiles of the MCG X-tiling array are represented with arrows and arrowhead indicating duplication at Xq28 and triplication at Xp22.2, respectively. The grey vertical lines represent the centromeric region for which no clones were available.**

performed an X-replication study with BrdU banding and FISH using a probe in dup(X)(q28). All carriers showed dominant inactivation of the duplicated allele (Supplementary eTable SIII). In Family 64-2-098 and Family 64-5-093, samples from the mother were not available for testing.

## DISCUSSION

We found dup(X)(q28) harboring *MECP2* in 3 of 115 (2.6%) male patients with MCA/ID and in 4 of 172 (2.3%) families affected by ID, through screening with in-house BAC-based arrays. Lugtenberg

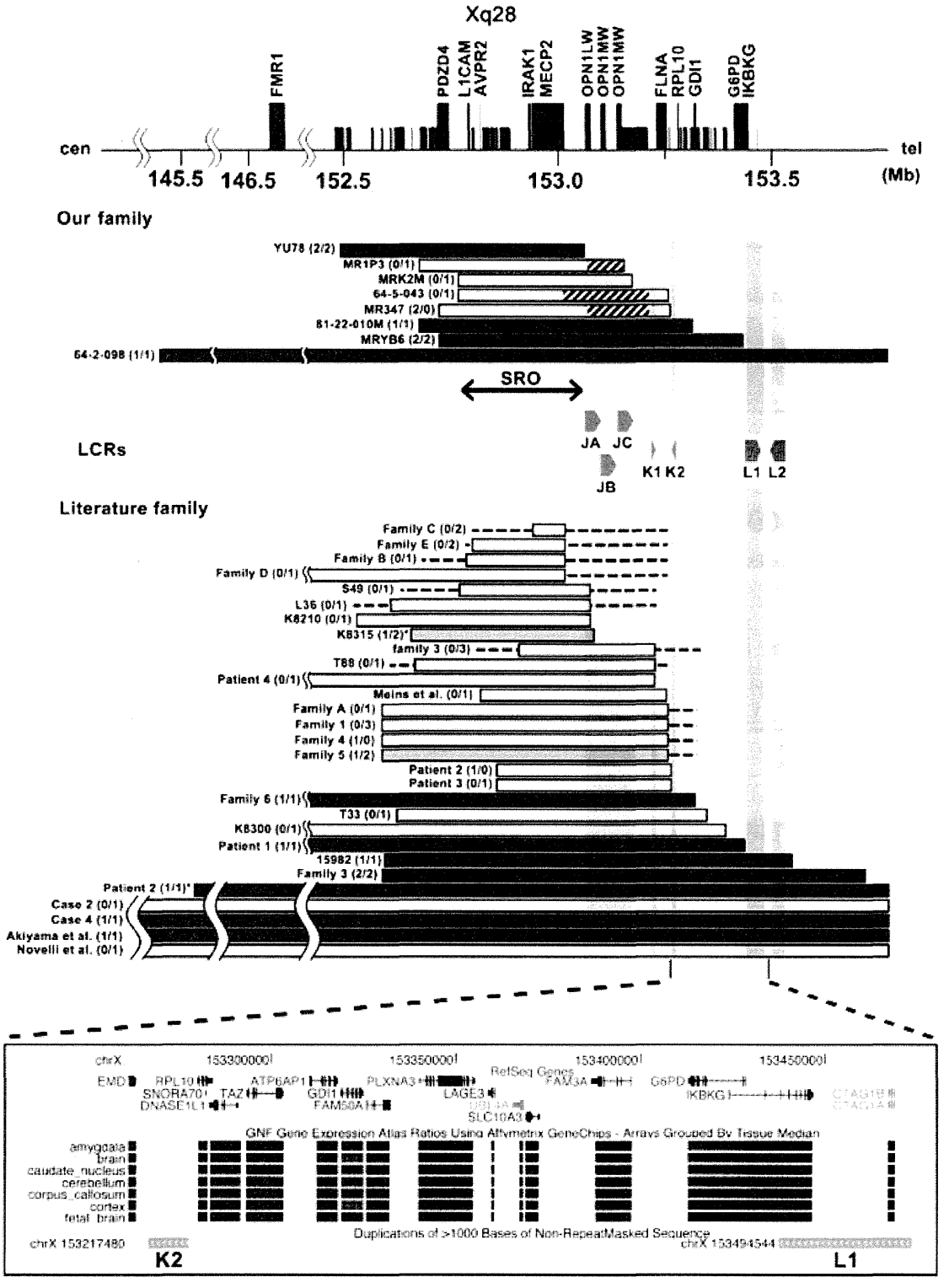
Xq28
FMR1
PDZD4
L1CAM
AVPR2
IRAK1
MECP2
OPN1LW
OPN1MW
OPN1MW
FLNA
RPL10
GDI1
G6PD
IKBKG
cen
tel
145.5
146.5
152.5
153.0
153.5
(Mb)
Our family
YU78 (2/2)
MR1P3 (0/1)
MRK2M (0/1)
64-5-043 (0/1)
MR347 (2/0)
81-22-010M (1/1)
MRYB6 (2/2)
64-2-098 (1/1)
SRO
LCRs
JA
JC
JB
K1
K2
L1
L2
Literature family
Family C (0/2)
Family E (0/2)
Family B (0/1)
Family D (0/1)
S49 (0/1)
L36 (0/1)
K8210 (0/1)
K8315 (1/2)*
family 3 (0/3)
T88 (0/1)
Patient 4 (0/1)
Meins et al. (0/1)
Family A (0/1)
Family 1 (0/3)
Family 4 (1/0)
Family 5 (1/2)
Patient 2 (1/0)
Patient 3 (0/1)
Family 6 (1/1)
T33 (0/1)
K8300 (0/1)
Patient 1 (1/1)
15982 (1/1)
Family 3 (2/2)
Patient 2 (1/1)*
Case 2 (0/1)
Case 4 (1/1)
Akiyama et al. (1/1)
Novelli et al. (0/1)
chrX
153300000
153350000
153400000
153450000
RefSeq Genes
EMD
RPL10
ATP6AP1
PLXNA3
FAM3A
G6PD
SNORA70
TAZ
GDI1
LAGE3
IKBKG
DNASE1L1
FAM50A1
SLC10A3
GNF Gene Expression Atlas Ratios Using Affymetrix GeneChips - Arrays Grouped By Tissue Median
amygdala
brain
caudate_nucleus
cerebellum
corpus_callosum
cortex
fetal_brain
Duplications of >1000 Bases of Non-RepeatMasked Sequence
chrX 153217480
chrX 153494544
K2
L1

FIG. 4.

TABLE II. Frequency of Hypoplasia of the Corpus Callosum in Our Patients and Reported Patients

| Refs. | Family name | Dup(X)(q28) including LCRL1 | |
|---|---|---|---|
| | | Yes | No |
| Our patients | Family 1–5, MR1P3, MR347, MRYB6 | 3/3 | 3/8 |
| Pai et al. [1997] [a] | K8300 | — | 0/1 |
| Lubs et al. [1999] [a] | K8210 | — | 0/1 |
| Goodman et al. [1998] | Cases 2 and 4 | 1/2 | — |
| Akiyama et al. [2001] | | 1/1 | — |
| Novelli et al. [2004] | | 0/1 | — |
| Meins et al. [2005] | | — | 0/1 |
| Van Esch et al. [2005] | S49, L36, T88, T33 | — | 0/4 |
| Rosenberg et al. [2005] [a] | 15982 | 1/1 | — |
| Friez et al. [2006] [a] | K8315 | — | 1/2[b] |
| Smyk et al. [2008] | Patient 2 (AS) | 1/1[b] | — |
| Lugtenberg et al. [2009] | Family A–E | — | 0/5 |
| Clayton-Smith et al. [2009] | Family 1, 3, 4, 5, 6 | 2/2 | 2/7 |
| Bartsch et al. [2009] | Patients 1–4 | 1/1 | 0/3 |
| Reardon et al. [2010] | Family 3 | — | 0/3 |
| Total | | 10/12 (83%) | 6/35 (17%) |

[a]Region of dup(X)(q28) were identified in Bauters et al.
[b]Agenesis of the corpus callosum.

et al. [2009] identified *MECP2* duplications in 3 of 283 (1.1%) males with unexplained XLID, suggesting that the frequency of *MECP2* duplications in males with ID is higher in Japan than in Western countries. In our study, dup(X)(q28) was inherited from the mother in all seven families for whom maternal DNA was available (Fig. 1).

Our aCGH analyses with the BAC-based X-tiling array and the oligonucleotide array showed that among the eight families, the dup(X)(q28) rearrangements varied in size with the SRO harboring at least 10 genes including *L1CAM* and *MECP2* according to the UCSC genome browser (Fig. 4). Although Family 64-2-098 had an ~9.4-Mb duplication encompassing 125 genes including *FMR1* and 21 miRNAs (Supplementary eFig. S2), the proband had approximately the same phenotype as the other patients with dup(X)(q28), indicating strongly that increased *MECP2* dosage is the primary contributor to the development of the salient clinical phenotypes. On the other hand, this proband exhibited short stature and facial dysmorphism not observed in our other patients with dup(X)(q28). Recently, a familial interstitial Xq27.3-q28 duplication encompassing the *FMR1* gene but not *MECP2* gene was found in patients with ID, short stature, hypogonadism, and facial dysmorphism [Rio et al., 2010], suggesting that the minimum common region proximal to *MECP2* within the duplications in these two families contributes to the short stature and facial dysmorphism phenotypes (Supplementary eFig. S2). A patient with a complex rearrangement including *MECP2* triplication was reported to have a severe phenotype [Carvalho et al., 2009]. Our aCGH analyses with the oligonucleotide array revealed duplications with embedded triplicated segments in 3 of the 8 families (37.5%; Fig. 4). The proband of Family 64-5-093 has a partial triplication of *MECP2*, but exhibits similar phenotypes to patients with duplication (Table I), suggesting that partial triplication of *MECP2* causes no increased *MECP2* dosage compared to duplication.

Twelve individuals from the eight families shared common phenotypes; severe ID (100%), muscular hypotonia (83%), absence of speech (100%), recurrent respiratory infections (83%), epilepsy

**FIG. 4. Schematic representation of dup(X)(q28) observed in our eight families and in the literature. Data are plotted in the order of the extent of distal duplication boundaries in our families and literature cases. A double-headed arrow indicates the smallest region of overlap (SRO) of our eight families containing 10 genes including *MECP2* and *L1CAM*. The position of genes at Xq28 was determined based on the UCSC genome browser (NCBI build 36 at the Genome Browser Gateway; http://genome.ucsc.edu/cgi-bin/hgGateway). The panel between our families and the literature families shows the position and direction of LCRs (JA, JB, JC, K1, K2, L1, L2). Filled bars and gray bars indicate families in which all patients and one of two siblings (Family 5 in the literature) showed hypoplasia of the corpus callosum (CC), respectively. Open bars represent families having no patients with hypoplasia of the CC. Asterisks indicate that patients showed agenesis of the CC. The shaded areas within each bar indicate triplication. Dashed lines indicate regions for which it was not determined whether they were duplicated or not in the original reports. The UCSC genome browser map represents the locus between LCRK2 and LCRL1. The expression levels in amygdala, brain, caudate nucleus, cerebellum, corpus callosum, cortex, and fetal brain are represented by expression data from GNF (The Genomics Institute of the Novartis Research Foundation) using Affymetrix GeneChips. Red indicates overexpression in the tissue, and green indicates underexpression.**

(75%), a round and expression-less face (83%), and apparent loss of cerebral volume (73%), similar to previous reports [del Gaudio et al., 2006; Bartsch et al., 2010; Ramocki et al., 2010] (Table I). Genotype–phenotype correlation among the 11 patients and 36 literature patients showed that 83% (10/12) of patients with distal breakpoints near/on/over LCRL exhibited hypoplasia of the CC, whereas only 17% (6/35) of those with breakpoints proximal to LCRL exhibited hypoplasia of the CC (Fig. 4; Table II). Precise mapping by real-time genomic PCR showed that the distal breakpoint of MRYB6 was located within *IKBKG* (data not shown), suggesting that copy-number gain of 13 genes between LCRK2 and LCRL1 is associated with hypoplasia of the CC. Hypoplasia of the CC is caused by processes that disrupt early anteroposterior and dorsoventral patterning to misspecification of midbrain or hindbrain germinal zones or due to degenerative processes [Chiappedi and Bejor, 2010]. In addition, an abnormal CC was reported in many severe disorders of midbrain–hindbrain development [Schell-Apacik et al., 2008]. Although the cause of hypoplasia of the CC cannot be identified with the resolution of MRI, hypoplasia of the CC is frequently associated with other brain anomalies. Among the 13 genes in our proposed critical interval, 8 genes (*ATP6AP*, *GDI1*, *FAM50A*, *PLXNA3*, *LAGE3*, *FAM3A*, *G6PD*, and *IKBKG*) show relatively high expression in brain tissue or in fetal brain (UCSC Genome Browser; Fig. 4). We cannot exclude the possibility that hypoplasia of the CC occurs secondary to *MECP2* overexpression but exhibits variable expressivity, but it is also possible that these genes or other genetic modifiers influence the penetrance/expressivity of hypoplasia of the CC. In particular, pathogenic mutations of *GDI1* (OMIM:300104) were found in two families with nonspecific ID [D'Adamo et al., 1998], and an identical 0.3 Mb region distal to *MECP2* at Xq28, containing *FLNA* and *GDI1* but not *MECP2* was identified in four unrelated families with ID [Vandewalle et al., 2009]. Defects in *IKBKG* (OMIM:300248) are the cause of incontinentia pigmenti (IP) (OMIM:308300), which is characterized by abnormalities of the skin, hair, eyes, nails, teeth, skeleton, heart, and central nervous system in females. Thus, overexpression of these two genes may contribute to hypoplasia of the CC. The proband in Family 64-2-098 with a large duplication encompassing 125 genes and 21 miRNAs showed the most severe developmental delay among our 12 cases, suggesting that there are other dosage-sensitive genes at Xq28 that are relevant to the degree of ID and neurodevelopmental delay as has been reported previously with large rearrangements [Sanlaville et al., 2009]. Taken together, our results indicate that the location of distal breakpoints and the size of the genomic rearrangements influence phenotypes caused by dup(X)(q28) encompassing *MECP2*.

In the proband of YU78, an ~228 kb triplication at Xp22.2, identified as a benign CNV in our previous study [Honda et al., 2010], was detected and FISH revealed that the trp(X)(p22.2) was inherited by the proband (II-3), his sister (II-1) and his brother (II-4) together with dup(X)(q28) after recombination during meiosis in the mother (Supplementary eFig. S3B). All carrier mothers showed skewed X-inactivation patterns and the chromosome carrying dup(X)(q28) was inactivated (Supplementary eTableSIII), suggesting trp(Xp22.2) to be a benign CNV.

Our data suggest that there is an association between the location of the distal breakpoint in *MECP2* duplication syndrome and the presence of hypoplasia of the CC. The CC is the largest transverse fiber tract that connects the two cerebral hemispheres and integrates motor sensory and cognitive performance of the brain [Aicardi et al., 1987]. Although agenesis of the CC (ACC) is one of the most common brain malformations observed in the general population (0.5 per 10,000 at autopsy) [Myrianthopoulos, 1977], the prevalence of ACC in children with developmental disabilities is much higher (230 per 10,000) [Jeret et al., 1985]. In addition, ACC is linked to various neuropsychiatric disorders, including attention-deficit hyperactivity disorder [Hynd et al., 1995] and schizophrenia [Lewis et al., 1988]. Furthermore, agenesis or hypoplasia of the CC is frequently associated with other structural abnormalities of the brain [Schell-Apacik et al., 2008; Chiappedi and Bejor, 2010]. Conventional karyotyping and/or array-CGH analyses using samples from patients with ACC identified candidate genes not only on chromosome 1 [Boland et al., 2007; van Bon et al., 2008; Caliebe et al., 2010], but also on chromosomes 3, 7, 8, 13, 15, 18, and 21 [Barkovich et al., 2009]. Therefore, the causes of ACC are heterogeneous, and in many instances, the specific gene alterations and developmental mechanisms are not well understood. Further studies are necessary to explore the cause of hypoplasia of the CC in this patient population, and determine the mechanism.

## ACKNOWLEDGMENTS

We thank the patients and families for their generous participation in this study, N. Murakami for cell culture and EBV-transformation, and M. Kato, A. Takahashi, and R. Mori for technical assistance. This study was supported by grants-in-aid for Scientific Research on Priority Areas and the Global Center of Excellence Program for Frontier Research on Molecular Destruction and Reconstitution of Tooth and Bone from the Ministry of Education, Culture, Sports, Science and Technology, Japan; by a grant from the New Energy and Industrial Technology Development Organization (NEDO); and, in part, by a research grant for Nervous and Mental Disorders from the Ministry of Health, Labor and Welfare, Japan. This study was also supported by the Joint Usage/Research of Medical Research Institute, Tokyo Medical Dental University. S. Honda is supported by a Research Fellowship of the Japan Society for the Promotion of Science (JSPS) for Young Scientists.

## REFERENCES

Aicardi J, Chevrie JJ, Barnton J. 1987. Agenesis of the corpus callosum. In: Myrianthopoulus NC, editor. Handbook of clinical neurology, Vol 6. Malformations. Amsterdam: Elsevier. pp 149–173.

Akiyama M, Kawame H, Ohashi H, Tohma T, Ohta H, Shishikura A, Miyata I, Usui N, Eto Y, 2001. Functional disomy for Xq26.3-qter in a boy with an unbalanced t(X;21)(q26.3;p11.2) translocation. Am J Med Genet 99:111–114.

Barkovich AJ, Millen KJ, Dobyns WB. 2009. A developmental and genetic classification for midbrain–hindbrain malformations. Brain 132: 3199–3230.

Bartsch O, Gebauer K, Lechno S, van Esch H, Froyen G, Bonin M, Seidel J, Thamm-Mucke B, Horn D, Klopocki E, Hertzberg C, Zechner U, Haaf T.

2010. Four unrelated patients with Lubs X-linked mental retardation syndrome and different Xq28 duplications. Am J Med Genet Part A 152A:305–312.

Boland E, Clayton-Smith J, Woo VG, McKee S, Manson FD, Medne L, Zackai E, Swanson EA, Fitzpatrick D, Millen KJ, Sherr EH, Dobyns WB, Black GC. 2007. Mapping of deletion and translocation breakpoints in 1q44 implicates the serine/threonine kinase AKT3 in postnatal microcephaly and agenesis of the corpus callosum. Am J Hum Genet 81: 292–303.

Caliebe A, Kroes HY, van der Smagt JJ, Martin-Subero JI, Tonnies H, van't Slot R, Nievelstein RA, Muhle H, Stephani U, Alfke K, Stefanova I, Hellenbroich Y, Gillessen-Kaesbach G, Hochstenbach R, Siebert R, Poot M, 2010. Four patients with speech delay, seizures and variable corpus callosum thickness sharing a 0.440 Mb deletion in region 1q44 containing the HNRPU gene. Eur J Med Genet 53:179–185.

Carvalho CM, Zhang F, Liu P, Patel A, Sahoo T, Bacino CA, Shaw C, Peacock S, Pursley A, Tavyev YJ, Ramocki MB, Nawara M, Obersztyn E, Vianna-Morgante AM, Stankiewicz P, Zoghbi HY, Cheung SW, Lupski JR. 2009. Complex rearrangements in patients with duplications of MECP2 can occur by fork stalling and template switching. Hum Mol Genet 18:2188–2203.

Chiappedi M, Bejor M. 2010. Corpus callosum agenesis and rehabilitative treatment. Ital J Pediatr 36:64.

Clayton-Smith J, Walters S, Hobson E, Burkitt-Wright E, Smith R, Toutain A, Amiel J, Lyonnet S, Mansour S, Fitzpatrick D, Ciccone R, Ricca I, Zuffardi O, Donnai D. 2009. Xq28 duplication presenting with intestinal and bladder dysfunction and a distinctive facial appearance. Eur J Hum Genet 17:434–443.

D'Adamo P, Menegon A, Lo Nigro C, Grasso M, Gulisano M, Tamanini F, Bienvenu T, Gedeon AK, Oostra B, Wu SK, Tandon A, Valtorta F, Balch WE, Chelly J, Toniolo D. 1998. Mutations in GDI1 are responsible for X-linked non-specific mental retardation. Nat Genet 19:134–139.

del Gaudio D, Fang P, Scaglia F, Ward PA, Craigen WJ, Glaze DG, Neul JL, Patel A, Lee JA, Irons M, Berry SA, Pursley AA, Grebe TA, Freedenberg D, Martin RA, Hsich GE, Khera JR, Friedman NR, Zoghbi HY, Eng CM, Lupski JR, Beaudet AL, Cheung SW, Roa BB. 2006. Increased MECP2 gene copy number as the result of genomic duplication in neurodevelopmentally delayed males. Genet Med 8:784–792.

Friez MJ, Jones JR, Clarkson K, Lubs H, Abuelo D, Bier JA, Pai S, Simensen R, Williams C, Giampietro PF, Schwartz CE, Stevenson RE. 2006. Recurrent infections, hypotonia, and mental retardation caused by duplication of MECP2 and adjacent region in Xq28. Pediatrics 118: e1687–1695.

Goodman BK, Shaffer LG, Rutberg J, Leppert M, Harum K, Gagos S, Ray JH, Bialer MG, Zhou X, Pletcher BA, Shapira SK, Geraghty MT. 1998. Inherited duplication Xq27-qter at Xp22.3 in severely affected males: Molecular cytogenetic evaluation and clinical description in three unrelated families. Am J Med Genet 80:377–384.

Hayashi S, Honda S, Minaguchi M, Makita Y, Okamoto N, Kosaki R, Okuyama T, Imoto I, Mizutani S, Inazawa J. 2007. Construction of a high-density and high-resolution human chromosome X array for comparative genomic hybridization analysis. J Hum Genet 52:397–405.

Hayashi S, Imoto I, Aizu Y, Okamoto N, Mizuno S, Kurosawa K, Honda S, Araki S, Mizutani S, Numabe H, Saitoh S, Kosho T, Fukushima Y, Mitsubuchi H, Endo F, Chinen Y, Kosaki R, Okuyama T, Ohki H, Yoshihashi H, Ono M, Takada F, Ono H, Yagi M, Matsumoto H, Makita Y, Hata A, Inazawa J. 2010. Clinical application of array-based comparative genomic hybridization by two-stage screening for 536 patients with mental retardation and multiple congenital anomalies. J Hum Genet 56:110–124.

Honda S, Hayashi S, Kato M, Niida Y, Hayasaka K, Okuyama T, Imoto I, Mizutani S, Inazawa J. 2007. Clinical and molecular cytogenetic characterization of two patients with non-mutational aberrations of the FMR2 gene. Am J Med Genet Part A 143:687–693.

Honda S, Hayashi S, Imoto I, Toyama J, Okazawa H, Nakagawa E, Goto Y, Inazawa J. 2010. Copy-number variations on the X chromosome in Japanese patients with mental retardation detected by array-based comparative genomic hybridization analysis. J Hum Genet 55:590–599.

Hynd GW, Hall J, Novey ES, Eliopulos D, Black K, Gonzalez JJ, Edmonds JE, Riccio C, Cohen M. 1995. Dyslexia and corpus callosum morphology. Arch Neurol 52:32–38.

Inazawa J, Azuma T, Ariyama T, Abe T. 1993. A simple G-banding technique adaptable for fluorescent in situ hybridization (FISH) and physical ordering of human renin (REN) and cathepsin E (CTSE) genes by multi-color FISH. Acta Histochem Cytochem 26:319–324.

Inazawa J, Inoue J, Imoto I. 2004. Comparative genomic hybridization (CGH)-arrays pave the way for identification of novel cancer-related genes. Cancer Sci 95:559–563.

Jeret JS, Serur D, Wisniewski K, Fisch C. 1985. Frequency of agenesis of the corpus callosum in the developmentally disabled population as determined by computerized tomography. Pediatr Neurosci 12:101–103.

Kubota T, Nonoyama S, Tonoki H, Masuno M, Imaizumi K, Kojima M, Wakui K, Shimadzu M, Fukushima Y. 1999. A new assay for the analysis of X-chromosome inactivation based on methylation-specific PCR. Hum Genet 104:49–55.

Lewis SW, Reveley MA, David AS, Ron MA. 1988. Agenesis of the corpus callosum and schizophrenia: A case report. Psychol Med 18:341–347.

Lubs H, Abidi F, Bier JA, Abuelo D, Ouzts L, Voeller K, Fennell E, Stevenson RE, Schwartz CE, Arena F. 1999. XLMR syndrome characterized by multiple respiratory infections, hypertelorism, severe CNS deterioration and early death localizes to distal Xq28. Am J Med Genet 85:243–248.

Lugtenberg D, Kleefstra T, Oudakker AR, Nillesen WM, Yntema HG, Tzschach A, Raynaud M, Rating D, Journel H, Chelly J, Goizet C, Lacombe D, Pedespan JM, Echenne B, Tariverdian G, O'Rourke D, King MD, Green A, van Kogelenberg M, Van Esch H, Gecz J, Hamel BC, van Bokhoven H, de Brouwer AP. 2009. Structural variation in Xq28: MECP2 duplications in 1% of patients with unexplained XLMR and in 2% of male patients with severe encephalopathy. Eur J Hum Genet 17:444–453.

Meins M, Lehmann J, Gerresheim F, Herchenbach J, Hagedorn M, Hameister K, Epplen JT. 2005. Submicroscopic duplication in Xq28 causes increased expression of the MECP2 gene in a boy with severe mental retardation and features of Rett syndrome. J Med Genet 42:e12.

Myrianthopoulos NC. 1977. Epidemiology of central nervous system malformations. In: Vinken PJ, Bruyn GW, Myrianthopoulos NC, editors. Congenital malformations of the brain and skull. Part I. Amsterdam: Elsevier. pp 139–171.

Novelli A, Bernardini L, Salpietro DC, Briuglia S, Merlino MV, Mingarelli R, Dallapiccola B. 2004. Disomy of distal Xq in males: Case report and overview. Am J Med Genet Part A 128A:165–169.

Pai GS, Hane B, Joseph M, Nelson R, Hammond LS, Arena JF, Lubs HA, Stevenson RE, Schwartz CE. 1997. A new X linked recessive syndrome of mental retardation and mild dysmorphism maps to Xq28. J Med Genet 34:529–534.

Ramocki MB, Tavyev YJ, Peters SU. 2010. The MECP2 duplication syndrome. Am J Med Genet Part A 152A:1079–1088.

Reardon W, Donoghue V, Murphy AM, King MD, Mayne PD, Horn N, Birk Moller L. 2010. Progressive cerebellar degenerative changes in the severe mental retardation syndrome caused by duplication of MECP2 and adjacent loci on Xq28. Eur J Pediatr 169:941–949.

Rio M, Malan V, Boissel S, Toutain A, Royer G, Gobin S, Morichon-Delvallez N, Turleau C, Bonnefont JP, Munnich A, Vekemans M,

Colleaux L. 2010. Familial interstitial Xq27.3q28 duplication encompassing the FMR1 gene but not the MECP2 gene causes a new syndromic mental retardation condition. Eur J Hum Genet 18:285–290.

Rosenberg C, Knijnenburg J, Chauffaille Mde L, Brunoni D, Catelani AL, Sloos W, Szuhai K, Tanke HJ, 2005. Array CGH detection of a cryptic deletion in a complex chromosome rearrangement. Hum Genet 116: 390–394.

Sanlaville D, Schluth-Bolard C, Turleau C. 2009. Distal Xq duplication and functional Xq disomy. Orphanet J Rare Dis 4:4.

Schell-Apacik CC, Wagner K, Bihler M, Ertl-Wagner B, Heinrich U, Klopocki E, Kalscheuer VM, Muenke M, von Voss H. 2008. Agenesis and dysgenesis of the corpus callosum: Clinical, genetic and neuroimaging findings in a series of 41 patients. Am J Med Genet Part A 146A:2501–2511.

Smyk M, Obersztyn E, Nowakowska B, Nawara M, Cheung SW, Mazurczak T, Stankiewicz P, Bocian E. 2008. Different-sized duplications of Xq28, including MECP2, in three males with mental retardation, absent or delayed speech, and recurrent infections. Am J Med Genet Part B 147B:799–806.

Takano K, Nakagawa E, Inoue K, Kamada F, Kure S, Goto Y. 2008. A loss-of-function mutation in the FTSJ1 gene causes nonsyndromic X-linked mental retardation in a Japanese family. Am J Med Genet Part B 147B: 479–484.

van Bon BW, Koolen DA, Borgatti R, Magee A, Garcia-Minaur S, Rooms L, Reardon W, Zollino M, Bonaglia MC, De Gregori M, Novara F, Grasso R, Ciccone R, van Duyvenvoorde HA, Aalbers AM, Guerrini R, Fazzi E, Nillesen WM, McCullough S, Kant SG, Marcelis CL, Pfundt R, de Leeuw N, Smeets D, Sistermans EA, Wit JM, Hamel BC, Brunner HG, Kooy F, Zuffardi O, de Vries BB. 2008. Clinical and molecular characteristics of 1qter microdeletion syndrome: Delineating a critical region for corpus callosum agenesis/hypogenesis. J Med Genet 45: 346–354.

Van Esch H, Bauters M, Ignatius J, Jansen M, Raynaud M, Hollanders K, Lugtenberg D, Bienvenu T, Jensen LR, Gecz J, Moraine C, Marynen P, Fryns JP, Froyen G. 2005. Duplication of the MECP2 region is a frequent cause of severe mental retardation and progressive neurological symptoms in males. Am J Hum Genet 77:442–453.

Vandewalle J, Van Esch H, Govaerts K, Verbeeck J, Zweier C, Madrigal I, Mila M, Pijkels E, Fernandez I, Kohlhase J, Spaich C, Rauch A, Fryns JP, Marynen P, Froyen G. 2009. Dosage-dependent severity of the phenotype in patients with mental retardation due to a recurrent copy-number gain at Xq28 mediated by an unusual recombination. Am J Hum Genet 85:809–822.

RESEARCH ARTICLE

AMERICAN JOURNAL OF medical genetics

# Ophthalmic Features of CHARGE Syndrome With CHD7 Mutations

**Sachiko Nishina,[1] Rika Kosaki,[2] Tatsuhiko Yagihashi,[3] Noriyuki Azuma,[1] Nobuhiko Okamoto,[4] Yoshikazu Hatsukawa,[5] Kenji Kurosawa,[6] Takahiro Yamane,[7] Seiji Mizuno,[8] Kinichi Tsuzuki,[9] and Kenjiro Kosaki[3,10]***

[1]Division of Ophthalmology, National Center for Child Health and Development, Tokyo, Japan

[2]Division of Medical Genetics, National Center for Child Health and Development, Tokyo, Japan

[3]Department of Pediatrics, Keio University School of Medicine, Tokyo, Japan

[4]Department of Medical Genetics, Osaka Medical Center and Research Institute for Maternal and Child Health, Osaka, Japan

[5]Department of Ophthalmology, Osaka Medical Center and Research Institute for Maternal and Child Health, Osaka, Japan

[6]Division of Medical Genetics, Kanagawa Children's Medical Center, Kanagawa, Japan

[7]Division of Ophthalmology, Kanagawa Children's Medical Center, Kanagawa, Japan

[8]Department of Genetics, Institute for Developmental Research, Aichi Human Service Center, Aichi, Japan

[9]Department of Ophthalmology, Aichi Children's Health and Medical Center, Aichi, Japan

[10]Center for Medical Genetrics, Keio University School of Medicine, Tokyo, Japan

Received 26 December 2010; Accepted 25 October 2011

Coloboma and various ocular abnormalities have been described in CHARGE syndrome, although the severity of visual impairment varies from case to case. We conducted a multicenter study to clarify the ophthalmic features of patients with molecularly confirmed CHARGE syndrome. Thirty-eight eyes in 19 patients with CHARGE syndrome and confirmed CHD7 mutations treated at four centers were retrospectively studied. Colobomata affected the posterior segment of 35 eyes in 18 patients. Both retinochoroidal and optic disk colobomata were bilaterally observed in 13 patients and unilaterally observed in 5 patients. The coloboma involved the macula totally or partially in 21 eyes of 13 patients. We confirmed that bilateral large retinochoroidal colobomata represents a typical ophthalmic feature of CHARGE syndrome in patients with confirmed CHD7 mutations; however, even eyes with large colobomata can form maculas. The anatomical severity of the eye defect was graded according to the presence of colobomata, macula defect, and microphthalmos. A comparison of the severity in one eye with that in the other eye revealed a low-to-moderate degree of agreement between the two eyes, reflecting the general facial asymmetry of patients with CHARGE syndrome. The location of protein truncation and the anatomical severity of the eyes were significantly correlated. We suggested that the early diagnosis of retinal morphology and function may be beneficial to patients, since such attention may determine whether treatment for amblyopia, such as optical correction and patching, will be effective in facilitating the visual potential or whether care for poor vision will be needed.
© 2012 Wiley Periodicals, Inc.

Key words:

How to Cite this Article:
Nishina S, Kosaki R, Yagihashi T, Azuma N, Okamoto N, Hatsukawa Y, Kurosawa K, Yamane T, Mizuno S, Tsuzuki K, Kosaki K. 2012. Ophthalmic features of CHARGE syndrome with CHD7 mutations.
Am J Med Genet Part A 158A:514–518.

## INTRODUCTION

CHARGE syndrome is a multiple malformation syndrome named from the acronym of its major features: coloboma, heart defects, atresia of the choanae, retarded growth and/or development, genital anomalies, and ear abnormalities [Pagon et al., 1981; Zentner et al., 2010]. The major ocular feature of CHARGE syndrome is coloboma, and a previous investigation by ophthalmologists revealed an incidence of up to 86%, although the severity

Grant sponsor: Ministry of Health, Labour and Welfare, Tokyo, Japan.
*Correspondence to:
Kenjiro Kosaki, M.D., Ph.D., Department of Pediatrics, Keio University School of Medicine, 35 Shinanomachi, Shinjuku-ku, Tokyo 160-8582, Japan. E-mail: kkosaki@z3.keio.ac.jp
Published online 2 February 2012 in Wiley Online Library (wileyonlinelibrary.com).
DOI 10.1002/ajmg.a.34400

of coloboma and visual impairment varied from case to case [Russell-Eggitt et al., 1990].

Recently, the gene *Chromodomain helicase DNA-binding protein-7* (*CHD7*) at chromosome 8q12.1 was identified as a causative gene of CHARGE syndrome [Vissers et al., 2004]. Up to 70% of patients clinically diagnosed as having CHARGE syndrome exhibit mutations in the *CHD7* gene [Aramaki et al., 2006a; Jongmans et al., 2006; Lalani et al., 2006]. Although the exact function of this gene product remains unknown, it may have an important effect on an early stage of ocular morphogenesis.

We conducted the present multicenter study to clarify the ophthalmic features of patients with molecularly confirmed CHARGE syndrome and to explore the role of *CHD7* in ocular development.

## PATIENTS AND METHODS

Thirty-eight eyes in 19 patients clinically diagnosed as having CHARGE syndrome at the National Center for Child Health and Development, the Osaka Medical Center and Research Institute for Maternal and Child Health, the Kanagawa Children's Medical Center, or the Institute for Developmental Research, Aichi Human Service Center were retrospectively studied. All the patients had been molecularly confirmed to carry *CHD7* mutations at the Keio University School of Medicine [Aramaki et al., 2006a]. The clinical diagnosis of CHARGE syndrome was made based on the Blake criteria [Blake et al., 1998]. Molecular screening for mutations in the *CHD7* gene was conducted as reported previously [Aramaki et al., 2006b]. Ophthalmic features were examined using slit-lamp biomicroscopy and binocular indirect ophthalmoscopy. Two patients were also examined using a spectral domain optical coherence tomography (SD-OCT). The SD-OCT images were obtained with RS-3000 (NIDEK Co., Ltd., Gamagori, Japan). The best-corrected visual acuity (BCVA) was measured with a standard Japanese VA chart using Landolt rings or pictures at 5 m, then converted to Snellen VA.

The anatomical severity of the eye defect was classified as follows: Grade 1, Normal; Grade 2, colobomata with macular formation; Grade 3, colobomata including the macula; and Grade 4, colobomata, macular defect, and microphthalmos. Then, Cohen's kappa coefficient [Cohen, 1960] was used to measure the agreement of the severity in the two eyes among 19 CHD7-mutation positive patients. The potential correlation between the anatomical severity of the eyes in an individual and the amino acid position where the truncation of the *CHD7* protein occurred in the same individual was evaluated among 14 patients with protein-truncating mutations.

This study was approved by the institutional ethics committee; the patients or the parents of the patients provided informed consent prior to enrollment in the study.

## RESULTS

The characteristics of the 38 eyes of the 19 patients with CHARGE syndrome carrying *CHD7* mutations are summarized in Table I. Ten patients (53%) were male and 9 (47%) were female. The age of the patients at the time of the examination ranged from 1 to 21 years (mean 7.9 ± 5.0 years). Ocular abnormalities were found in 18 patients (94.7%), bilateral abnormalities were observed in 17 patients (89.4%), and unilateral abnormalities were observed in 1 patient (5.3%). Among these 18 patients, all 35 abnormal eyes had varying severities of colobomata.

TABLE I. Characteristics of Patients of CHARGE Syndrome With CHD7 Mutations (n = 9)

| Variable | Number |
|---|---|
| Gender | |
| Male | 10 (53%) |
| Female | 9 (47%) |
| Age at examination | 1–21 years |
| Mean | 7.9 ± 5.0 years |
| Ocular abnormalities (colobomata) | |
| Bilateral | 17 (89.4%) |
| Unilateral | 1 (5.3%) |
| None | 1 (5.3%) |
| BCVA | |
| <20/400 | 4 (21.1%) |
| 20/400 to <20/60 | 7 (36.8%) |
| 20/60 to 20/20 | 6 (31.6%) |
| Not measured | 2 (10.5%) |

BCVA, best-corrected visual acuity.

The ocular features of the individual patients are summarized in Table II. Colobomata affected the posterior segment in 35/38 eyes (92.1%), retinochoroidal coloboma was present in 33 eyes (86.8%), and optic disk coloboma was present in 33 eyes (86.8%). Both retinochoroidal coloboma and optic disk coloboma were bilaterally present in 15 patients (78.9%) and unilaterally present in 3 patients (15.8%). The coloboma involved the macula totally or partially in 21 eyes (55.3%) of the 13 patients (68.4%): bilaterally in 8 patients

TABLE II. Ocular Features of the Patients (n = 19 patients, 38 eyes)

| | Number of patients (%) | | | |
|---|---|---|---|---|
| Findings | Bilateral | Unilateral | Total | Number of eyes (%) |
| Colobomata | 17 (89.5) | 1 (5.3) | 18 (94.7) | 35 (92.1) |
| Retinochoroidal | 15 (78.9) | 3 (15.8) | 18 (94.7) | 33 (86.8) |
| Optic disk | 15 (78.9) | 3 (15.8) | 18 (94.7) | 33 (86.8) |
| Macula | 8 (42.1) | 5 (26.3) | 13 (68.4) | 21 (55.3) |
| Iris | 1 (5.3) | 0 (0.0) | 1 (5.3) | 2 (5.3) |
| Lens | 0 (0.0) | 1 (5.3) | 1 (5.3) | 1 (2.6) |
| Microphthalmos | 3 (15.8) | 2 (10.5) | 5 (26.3) | 8 (21.1) |
| Microcornea | 3 (15.8) | 1 (5.3) | 4 (21.1) | 7 (18.4) |
| Ptosis | 1 (5.3) | 1 (5.3) | 2 (10.5) | 3 (7.9) |
| PFV | 0 (0.0) | 1 (5.3) | 1 (5.3) | 1 (2.6) |
| Cataract | 0 (0.0) | 1 (5.3) | 1 (5.3) | 1 (2.6) |
| High myopia (>6.0 D) | 2 (10.5) | 1 (5.3) | 3 (15.8) | 5 (13.2) |

PFV, persistent fetal vasculature.

(42.1%) and unilaterally in 5 patients (26.3%). The SD-OCT demonstrated a partially formed macula and cystic changes in the colobomatous area in 1 case (Fig. 1).

Only 2 eyes of 1 patient (5.3%) were identified as having iris colobomata, and 1 eye (2.6%) of another patient was revealed by examination under general anesthesia to have a dislocated and colobomatous lens. No cases of eyelid colobomata were seen, but congenital ptosis was present in 3 eyes (7.9%) of 2 patients who had undergone surgical treatment. All the cases of ptosis were not pseudoptosis associated with microphthalmos and/or cranial nerve palsy, but were true congenital ptosis associated with poor levator function. We evaluated the levator muscle function in each case. None of the patients had a history of acquired causes or signs of oculomotor palsy, such as paralytic strabismus and limited ocular movement.

Microphthalmos was found in 8 eyes (21.1%) of 5 patients (26.3%): bilaterally in 3 patients (15.8%) and unilaterally in 2 patients (10.5%). Microcornea was also present in 7 eyes (18.4%) of 4 patients (21.1%): bilaterally in 3 patients (15.8%) and unilaterally in 1 patient (5.3%). Persistent fetal vasculature was identified in 1 eye (2.6%). Cataracts had developed in 1 eye (2.6%), but neither glaucoma nor retinal detachment was observed in this series.

The refraction could be estimated in 23 eyes of 12 patients (63.2%). Of these eyes, 10 were myopic, 7 were emmetropic, and 6 were hypermetropic. High myopia (−6.00 diopters or more) was found in 5 eyes (13.2%) of 3 patients (15.8%).

The BCVA are shown in Table I. The measurement of VA was possible in 17 patients (89.5%) older than 3 years of age. The remaining 2 patients were infants or mentally retarded. The binocular BCVA or BCVA in the better eye was less than 20/400 in 4 patients (21.1%), less than 20/60 but no less than 20/400 in 7 patients (36.8%), and 20/60 to 20/20 in 6 patients (31.6%) with macular formation (Fig. 1). The overall prevalence of blindness and visual impairment (less than 20/60) [World Health Organization, 1992] among the 17 patients was 65%.

The agreement of anatomical severity between the 2 eyes in each of the 19 patients was evaluated using Cohen's Kappa statistics. The $\kappa$ statistic of 0.41 suggested a moderate degree of agreement, per the guidelines by Landis and Koch [1977]. Because there was a moderate, if not a substantial, agreement between the severity of the 2 eyes, the severity grading of the more severely affected eye was used as the representative grade for the severity of the eyes in an individual. The correlation between the anatomical severity of the eyes in an individual and the amino acid position where the truncation of the CHD7 protein occurred in the same individual is illustrated in Figure 2. Patients with truncated protein devoid of the SANT domain tended to have severer anatomical defects of the eyes. Subcategorization of the patients according to the presence or absence of the SANT domain (4 cases with intact SANT domain and 10 other cases), and the subcategorization of the anatomical severity of the eyes in an individual (7 cases classified as Grade 1 or 2 vs. 7 cases classified as Grade 3 or 4) revealed a statistically

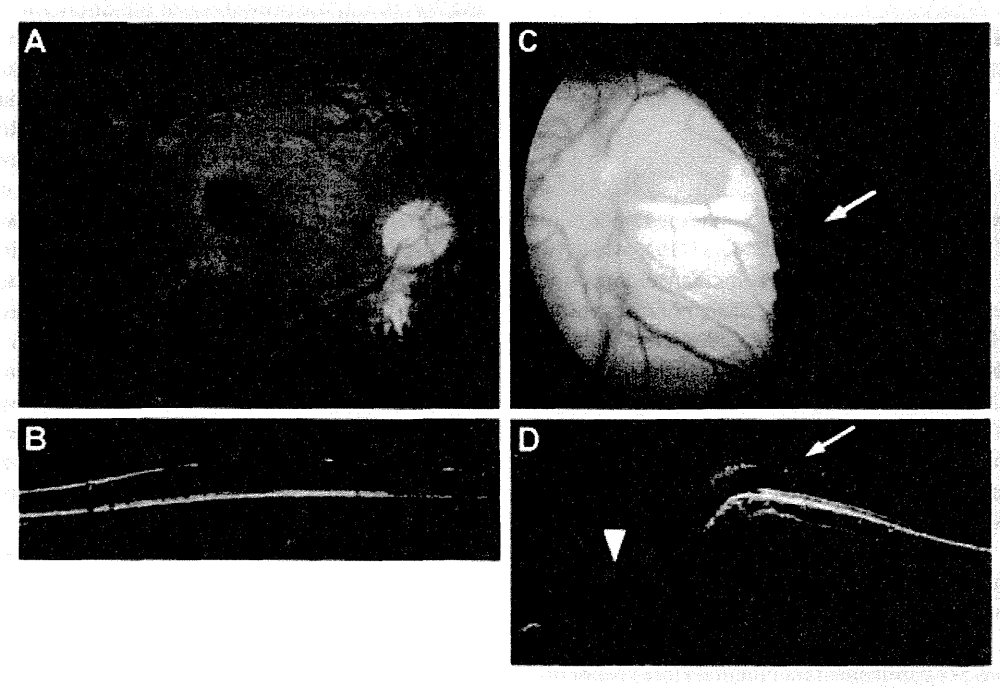


**FIG. 1. Fundus photographs and spectral domain optical coherence tomography (SD-OCT) scan of the retina in the right eye (A,B) and the left eye (C,D) in a 6-year-old girl. A: Retinochoroidal colobomata inferior to the optic disk is visible in the right eye. B: The SD-OCT shows a good macular formation in the right eye, resulting in a BCVA of 20/20. C: Retinochoroidal and optic disk coloboma are seen in the left eye. The colobomata partially involved the macula (arrow). D: The SD-OCT shows a partially formed macula (arrow) and cystic changes in the colobomatous area (arrow head) in the left eye, resulting in a BCVA of 20/50 after ambiyopia treatment.**

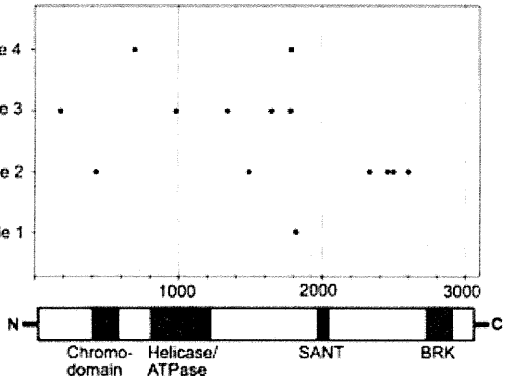


**FIG. 2. The correlation between the anatomical severity of the eyes in an individual and the amino acid position where the truncation of the CHD7 protein occurred in the same individual. Horizontal axis indicates amino acid position of the CHD7 protein together with the domains of the protein. Vertical axis indicates the anatomical severity of the eye defect classified as follows: Grade 1, Normal; Grade 2, colobomata with macular formation; Grade 3, colobomata including the macula; and Grade 4, colobomata, macular defect, and microphthalmos.**

significant correlation between the location of protein truncation and the anatomical severity of the eyes ($P = 0.02$, chi-squared test).

## DISCUSSION

In the current series, the incidence of coloboma, the major ocular feature of CHARGE syndrome, was 94.7% (18/19), which was much higher than the previously reported incidence. Since most of the authors were ophthalmologists, the number of cases without eye defects might have been underrepresented. Hence, this high incidence should be viewed with caution. Nevertheless, attending clinical geneticists were on duty at all the participating children's hospitals, and thus the bias from such underrepresentation may be relatively small. The finding that there was one mutation-positive patient who did not have abnormal eye findings confirms that no finding in CHARGE syndrome has a 100% penetrance as is sometimes surmised.

Both retinochoroidal and optic disk coloboma occurred in 94.7% of the cases, mostly bilaterally, while the incidence of iris coloboma was only 5.3% (1/19). Coloboma also affected the macula in 68.4% of the cases. We confirmed that bilateral large retinochoroidal colobomata represent a typical ophthalmic feature of CHARGE syndrome with *CHD7* mutations.

The incidence of anomalies in the anterior segment was lower than that in the posterior segment, although microphthalmos, microcornea, PFV, and cataracts were present in some cases bilaterally or unilaterally. The presence of characteristic large retinochoroidal coloboma indicates the essential role of *CHD7* in the closure of the fetal fissure posteriorly between 5 and 6 weeks of gestation, and the malfunction of *CHD7* may have an effect so severe as to influence the entire ocular morphogenesis to some degree. Although most cases had bilateral colobomata in the posterior segment, the severity and associated features often differed between the two eyes. Other associated features in this series were ptosis in 10.5% and high myopia in 15.8%. Subtle-associated anomalies and refractive errors may have been underestimated in examinations that were not performed under general anesthesia.

The anatomical severity grading of the eye defect was evaluated in two ways: a comparison between the severity in one eye in comparison with that in the other eye and the correlation between the severity and the genotype. The low-to-moderate degree of agreement between the two eyes (i.e., left and right) reflects the general facial asymmetry in patients with CHARGE syndrome [Zentner et al., 2010]. In other words, the lack of substantial or perfect agreement between the anatomical severity of the right and the left eyes indicates a variable phenotypic effect of the same mutation. Yet, the location of protein truncation and the anatomical severity of the eyes were significantly correlated: if the chromodomain, helicase/ATP domain, and SANT domains are intact, the severity of the eyes tends to be milder. Interestingly, all four cases in which those domains were intact had less severe eye defects with intact macula. Further studies are warranted to verify this potential genotype–phenotype correlation.

The visual acuities of the eyes ranged between no light perception and 20/20, and the prevalence of blindness and visual impairment (less than 20/60) was 65% among 17 patients. A poor visual prognosis depended on the presence of a large coloboma involving the macula in the posterior segment and associated microphthalmos or microcornea, as reported previously [Russell-Eggitt et al., 1990; Hornby et al., 2000]. On the other hand, even eyes with large colobomata as a result of *CHD7* mutations were capable of forming maculas, resulting in good central visual acuity with superior visual field defects. As shown in the case illustrated in Figure 1, even a partially formed macula will enable useful vision following the adequate treatment of amblyopia as optical correction and patching during the earlier age of visual development. A recent report of a case examined using OCT revealed additional morphologic characteristics of eyes in patients with CHARGE syndrome carrying *CHD7* mutations [Holak et al., 2008]. Further investigation of retinal morphology and function using OCT and electroretinograms (ERG) may help to clarify the function of *CHD7* in ocular morphogenesis, including macular formation.

We suggested that the early diagnosis of retinal morphology and function, especially of macular lesions by way of OCT and ERG, may be beneficial to patients, since such attention may determine whether treatment for amblyopia, such as optical correction and patching, will be effective in facilitating the visual potential or whether care for poor vision will be needed. An infant's visual acuity rapidly develops during its first 2–3 years and continues up until 7–8 years of age, but plasticity decreases progressively thereafter. Thus, a better visual prognosis can be obtained with the earlier treatment of amblyopia during the critical period of visual development.

## ACKNOWLEDGMENTS

This study was supported by the Health and Labour Sciences Research Grants of Research on Intractable Diseases from the Ministry of Health, Labour and Welfare, Tokyo, Japan.

## REFERENCES

Aramaki M, Udaka T, Kosaki R, Makita Y, Okamoto N, Yoshihashi H, Oki H, Nanao K, Moriyama N, Oku S, Hasegawa T, Takahashi T, Fukushima Y, Kawame H, Kosaki K. 2006a. Phenotypic spectrum of CHARGE syndrome with CDH7 mutations. J Pediatr 148:410–414.

Aramaki M, Udaka T, Torii C, Samejima H, Kosaki R, Takahashi T, Kosaki K. 2006b. Screening for CHARGE syndrome mutations in the CDH7 gene using denaturing high-performance liquid chromatography. Genet Test 10:244–251.

Blake KD, Davenport SL, Hall BD, Hefner MA, Pagon RA, Williams MS, Lin AE, Graham JM Jr. 1998. CHARGE association: An update and review for the primary pediatrician. Clin Pediatr (Phila) 37:159–173.

Cohen J. 1960. A coefficient of agreement for nominal scales. Educ Psychol Meat 20:37–46.

Holak HM, Kohlhase J, Holak SA, Holak NH. 2008. New recognized ophthalmic morphologic anomalies in CHARGE syndrome caused by the R2319C mutation in the CHD7 gene. Ophthalmic Genet 29:79–84.

Hornby SJ, Adolph S, Girbert CE, Dandona L, Foster A. 2000. Visual acuity in children with coloboma. Clinical features and a new phenotypic classification system. Ophthalmology 107:511–520.

Jongmans MC, Admiraal RJ, van der Donk KP, Vissers LE, Baas AF, Kapusta L, van Hagen JM, Donnai D, de Ravel TJ, Veltman JA, van Kessel AG, De Vries BB, Brunnaer HG, Hoefsloot LH, van Ravenswaaj CM. 2006. CHARGE syndrome: The phenotypic spectrum of mutations in the CHD7 gene. J Med Genet 43:306–314.

Lalani SR, Saliullah AM, Fernbach SD, Harutyunyan KG, Thaller C, Peterson LE, McPherson JD, Gibbs RA, White LD, Hefner M, Davenport SLH, Graham JM Jr, Bacino CA, Glass NL, Towbin JA, Craigen WJ, Neish SR, Lin AE, Belmont JW. 2006. Spectrum of CHD7 mutations in 110 individuals with CHARGE syndrome and genotype–phenotype correlation. Am J Hum Genet 78:303–314.

Landis JR, Koch GG. 1977. The measurement of observer agreement for categorical data. Biometrics 33:159–174.

Pagon RA, Graham JM Jr, Zonana J, Yong SL. 1981. Coloboma, congenital heart disease, and choanal atresia with multiple anomalies: CHARGE association. J Pediatr 99:223–227.

Russell-Eggitt IM, Blake KD, Taylor DSI, Wyse RKH. 1990. The eye in the CHARGE association. Br J Ophthalmol 74:421–426.

Vissers LE, van Ravenswaaij CM, Admiraal R, Hurst JA, de Vries BB, Janssen IM, van der Vliet WA, Huys EH, de Jong PJ, Hamel BC, Schoenmakers EF, Brunner HG, Veltman JA, van Kessel AG. 2004. Mutations in a new member of the chromodomain gene family cause CHARGE syndrome. Nat Genet 36:955–957.

World Health Oraganization. 1992. International statistical classification of diseases and related problems. 10th revision. Vol. 1. Geneva, Switzerland: World Health Organization.

Zentner GE, Layman WS, Martin DM, Scacheri PC. 2010. Molecular and phenotypic aspects of CHD7 mutation in CHARGE syndrome. Am J Med Genet Part A 152A:674–686.

RESEARCH ARTICLE

AMERICAN JOURNAL OF medical genetics PART A

# *MBTPS2* Mutation Causes BRESEK/BRESHECK Syndrome

**Misako Naiki,[1,2] Seiji Mizuno,[3] Kenichiro Yamada,[1] Yasukazu Yamada,[1] Reiko Kimura,[1] Makoto Oshiro,[4] Nobuhiko Okamoto,[5] Yoshio Makita,[6] Mariko Seishima,[7] and Nobuaki Wakamatsu[1]***

[1]Department of Genetics, Institute for Developmental Research, Aichi Human Service Center, Kasugai, Aichi, Japan

[2]Department of Pediatrics, Nagoya University Graduate School of Medicine, Nagoya, Aichi, Japan

[3]Department of Pediatrics, Central Hospital, Aichi Human Service Center, Kasugai, Aichi, Japan

[4]Department of Pediatrics, Japanese Red Cross Nagoya Daiichi Hospital, Nagoya, Aichi, Japan

[5]Department of Medical Genetics, Osaka Medical Center and Research Institute for Maternal and Child Health, Izumi, Osaka, Japan

[6]Education Center, Asahikawa Medical University, Asahikawa, Hokkaido, Japan

[7]Department of Dermatology, Gifu University Graduate School of Medicine, Gifu, Gifu, Japan

Received 25 July 2011; Accepted 17 October 2011

BRESEK/BRESHECK syndrome is a multiple congenital malformation characterized by brain anomalies, intellectual disability, ectodermal dysplasia, skeletal deformities, ear or eye anomalies, cleft palate or cryptorchidism, and renal anomalies or small kidneys, with or without Hirschsprung disease and cleft palate or cryptorchidism. This syndrome has only been reported in three male patients. Here we report on the fourth male patient presenting with brain anomaly, intellectual disability, growth retardation, ectodermal dysplasia, vertebral skeletal anomaly, Hirschsprung disease, low set and large ears, cryptorchidism, and small kidneys. These manifestations fulfill the clinical diagnostic criteria of BRESHECK syndrome. Since all patients with BRESEK/BRESHECK syndrome are male, and X-linked syndrome of ichthyosis follicularis with atrichia and photophobia is sometimes associated with several features of BRESEK/BRESHECK syndrome such as intellectual disability, vertebral and renal anomalies, and Hirschsprung disease, we analyzed the causal gene of ichthyosis follicularis with atrichia and photophobia syndrome, *MBTPS2*, in the present patient and identified an p.Arg429His mutation. This mutation has been reported to cause the most severe type of ichthyosis follicularis with atrichia and photophobia syndrome, including neonatal and infantile death. These results demonstrate that the p.Arg429His mutation in *MBTPS2* causes BRESEK/BRESHECK syndrome. © 2011 Wiley Periodicals, Inc.

Key words: BRESEK/BRESHECK syndrome; ichthyosis follicularis with atrichia and photophobia syndrome; *MBTPS2*

How to Cite this Article:
Naiki M, Mizuno S, Yamada K, Yamada Y, Kimura R, Oshiro M, Okamoto N, Makita Y, Seishima M, Wakamatsu N. 2012. *MBTPS2* mutation causes BRESEK/BRESHECK syndrome.
Am J Med Genet Part A 158A:97–102.

## INTRODUCTION

BRESEK/BRESHECK syndrome (OMIM# 300404), a multiple congenital malformation disorder characterized by brain anomalies, intellectual disability, ectodermal dysplasia, skeletal deformities, Hirschsprung disease, ear or eye anomalies, cleft palate or cryptorchidism, and kidney dysplasia/hypoplasia [Reish et al., 1997]. The acronym BRESEK refers to the common findings, whereas BRESHECK refers to all manifestations. Because the first two patients were maternally related half brothers, an X-linked disorder was proposed. Although each symptom of these patients is often observed in other congenital diseases, the combination of all symptoms is rare, and only one additional patient with BRESEK has been reported to date [Tumialán and Mapstone, 2006]. Here, we present the fourth male patient with multiple anomalies. The patient presented with a variety of clinical features that were consistent with those of the previously reported BRESHECK syndrome.

The syndrome of ichthyosis follicularis with atrichia and photophobia (IFAP, OMIM# 308205), an X-linked recessive oculocutaneous disorder, is characterized by a peculiar triad of ichthyosis follicularis, total or subtotal atrichia, and varying degrees

Grant sponsor: Takeda Science Foundation; Grant sponsor: Health Labour Sciences Research Grant.

*Correspondence to:
Nobuaki Wakamatsu, Department of Genetics, Institute for Developmental Research, Aichi Human Service Center, 713-8 Kamiya-cho, Kasugai, Aichi 480-0392, Japan. E-mail: nwaka@inst-hsc.jp

Published online 21 November 2011 in Wiley Online Library (wileyonlinelibrary.com).
DOI 10.1002/ajmg.a.34373